UiT
THE ARCTIC
UNIVERSITY
OF NORWAY

Department of Physics and Technology, Faculty of Science and Technology

Carbon Nanotube Spectrally Selective Solar Thermal Absorbers

Zhonghua Chen

A dissertation for the degree of Philosophiae Doctor – October 2016

Abstract

A solar absorber is the essential component in solar thermal collectors being used to absorb and convert solar radiation into heat. In order to be optically and thermally efficient, the solar absorber should be spectrally selective, i.e. a high solar absorption in the solar spectrum and a low thermal emittance in the IR wavelength region. The manufacturing cost for high performance of spectrally selective absorbers is high and needs to be further reduced in order to improve the cost-competitiveness of solar thermal collectors. Additionally, there are demands for more environmentally friendly utilization of solar energy, such as reducing the amount of toxic chemicals and heavy metals involved, reducing the energy demand during manufacturing and increasing long term durability.

The main objectives of this work were to investigate a) the feasibility of depositing multi-walled carbon nanotubes (MWCNTs) homogeneously on metal substrates by electrophoresis and b) the performance of MWCNT coatings as spectrally selective absorbers. Stable aqueous MWCNT suspensions were prepared and employed in electrophoretic deposition (EPD) of MWCNT coatings on aluminum substrates. The surface morphologies of MWCNT coatings were examined. Spectral reflectance of the MWCNT absorbers was measured to assess their spectral selectivity. Accelerated ageing tests on the MWCNT absorbers were carried out in order to evaluate long-term durability.

The deposited MWCNT coatings are homogeneous and exhibit good spectral selectivity combined with the underlying aluminum substrate. The best MWCNT absorber spectral selectivity achieved was a solar absorptance of 0.90 and a thermal emittance of 0.13 which are slightly under par with the performance of currently available commercial absorber products. Accelerated ageing tests revealed that MWCNT absorbers had an excellent thermal stability however it was not resistant to damage from condensation. Therefore, silica/silica-titania thin films were coated on top of the MWCNT coating as a protective layer. The protective films had little impact on the spectral selectivity of MWCNT absorbers and improved the long-term durability significantly. After 600 hours of testing, the performance criterion (PC) value was lower than 0.015, which confirms that the MWCNT absorbers coated with protective films can be qualified according to ISO 22975-3.

Keywords: Solar absorbers; Thermal; Spectral selectivity; Carbon nanotube; Electrophoretic deposition; Durability

List of papers

I. Zhonghua Chen, Tobias Boström. Electrophoretically deposited carbon nanotube spectrally selective solar absorbers. Solar Energy Materials & Solar Cells. 144 (2016) 678–683

II. Zhonghua Chen, A. Jain, T. Boström, Simulation of Anti-reflection coated carbonaceous spectrally selective absorbers. Energy Procedia. 58 (2014) 179 – 184

III. Zhonghua Chen, Quang Hong Nguyen, Tobias Boström. Carbon Nanotube Spectrally Selective Solar Absorbers. Eurosun Conference Proceedings. doi:10.18086/eurosun.2014.03.05

IV. Zhonghua Chen, Tobias Boström. Anti-reflection Coated Spectrally Selective Carbon Nanotube Solar Absorbers. Renewable Energy and Environmental Sustainability 1, 2 (2016)

V. Zhonghua Chen, Tobias Boström. Accelerated ageing tests of carbon nanotube spectrally selective solar absorbers. Solar Energy Materials & Solar Cells 157 (2016) 777–782

Brief description of the papers

Paper I

An investigation of three types of carbon nanotubes (CNT) coatings electrophoretically deposited on aluminum substrates for use as spectrally selective solar thermal absorbers is reported. Stable aqueous CNT suspensions were used for electrophoretic deposition. The CNT coatings after heat treatment were visibly uniform. The CNT coating thickness, surface morphology and reflectance of CNT absorbers were characterized by White Light Interferometry, Scanning Electron Microscopy and Spectrophotometry, respectively. The effect of CNT coating thickness, deposition parameters and peak heat treatment temperature on the spectral selectivity was reported. The achieved solar absorptance and thermal emittance with the optimal spectral selectivity were 0.79 and 0.14 for the T-CNT absorber, 0.90 and 0.14 for the N-CNT absorber, 0.90 and 0.13 for the P-CNT absorber.

Paper II

The potential of three carbonaceous materials, graphite, soot and single-walled carbon nanotubes (SWCNT) as spectrally selective absorbers has been evaluated using the thin film simulation software Setfos. Aluminum was chosen as the substrate material. To further enhance the spectral selectivity of the solar absorbers, simulations with an anti-reflection (AR) layers consisting of alumina or silica were also performed. Soot and SWCNT exhibit good spectral selectivity without an added AR layer, graphite does not. The best selectivity with AR layer was achieved for a soot absorber coated with a thin silica layer.

Paper III

Carbon nanotube (CNT) layers were coated by electrophoretic deposition (EPD) on aluminum substrates. Stable aqueous CNT suspensions consisted of multi-walled CNTs, DI water and surfactant was used for EPD. Various thicknesses and compositions of homogenous CNT coatings were prepared by tuning the electrophoretic parameters, such as voltage, inter-electrode spacing and deposition time. A voltage threshold of 15 V for uniform CNT deposition was discovered for the used aqueous CNT suspension. With thicker CNT coatings, the absorption increased in both visible and IR spectral range. Higher peak temperatures of heat treatment resulted in a lower thermal emittance without decreasing the solar absorptance; hence the spectral selectivity of CNT absorbers was improved. The results have indicated CNTs as a promising material for spectrally selective solar absorbers.

Paper IV

The paper reports the work of improving spectral selectivity of previously fabricated multi-walled carbon nanotube (MWCNT) solar absorbers. Porous silica as anti-reflection layer was spin-coated on top of MWCNT coatings. The precursor solution of porous silica was prepared using tetraethylorthosilicate (TEOS), and PF127 was used as a pore-forming agent. A maximum solar absorptance gain of 0.02 was achieved, which improved the spectral selectivity of MWCNT absorbers. The effect of the anti-reflection layer depends on not only its thickness/refractive index but also the roughness of the aluminum substrate.

Paper V

Accelerated ageing tests of previously produced novel multi-walled carbon nanotube (MWCNT) spectrally selective absorbers are presented. The procedure for performing the tests of condensation resistance and thermal stability followed the recommendations in the international standard ISO 22975-3: Absorber surface durability. The primary results revealed that the MWCNT absorber had a good

thermal stability but was not resistant to condensation. Therefore, different types of thin films such as dense silica, silica-titania were deposited on top of MWCNT absorbers as protective layer to prevent the penetration of condensed water. Although all MWCNT absorbers coated with protective layer had little or no gain in spectral selectivity compared to those without protective layer, accelerated ageing tests indicated that the long-term durability was significantly improved.

Comments on my contribution

I am responsible for the major part of the writing in all the above publications, prepared all samples and performed all experiments and measurements apart from the parts mentioned below:
FTIR measurements on the samples on which condensation and thermal stability tests had been performed were made by Øystein Jordheim.
SEM was operated by Tom-Ivar Eilertsen.
Matlab codes for generating reflectance curves and the calculation of solar absorptance and thermal emittance values were programmed by Dilip Chithambaranadhan.

Contents

List of symbols and constants

α	Normal solar absorptance
$A(\lambda)$	Absorptance
B_λ	Radiance at the wavelength of λ, W sr^{-1} m^{-3}
c	Speed of light in vacuum, m/s
ε	Normal thermal emittance
E_0	Initial amplitude of electric field
$E(x,t)$	Amplitude of electric field at the time t and the position x
$e(\lambda)$	Emittance
h	Planck's constant
I_{sol}	Spectral solar irradiance, W sr^{-1} m^{-3}
I_p	Thermal radiance, W sr^{-1} m^{-3}
k	The imaginary part of refractive index/the extinction coefficient
k_B	Boltzmann's constant
λ	Wavelength, μm
n	The real part of refractive index
N	Complex refractive index
ζ	Zeta potential, mV
$R(\lambda)$	Reflectance
t	Dwell time at T_{p}, minutes
T	Absolute temperature, K
$T(\lambda)$	Transmittance
$T_{\max}$	Maximum operation temperature corresponded to solar absorptance and thermal emittance, ℃
T_{p}	Peak temperature during heat treatment, ℃
ω	Angular frequency

Abbreviations

AC	Alternating Current
AM	Air mass
AR	Anti-reflection
CNT	Carbon nanotube
CTAB	Hexadecyltrimethylammonium bromide
DC	Direct Current
DHW	Domestic hot water system
DI	Deionized
EPD	Electrophoretic deposition
EDS	Energy-dispersive X-ray spectroscopy
EtOH	Ethanol
IEA	International Energy Agency
ISO	International Organization for Standardization
ITO	Indium tin oxide
IR	Infrared
MTES	Methyltrietoxysilane
MWCNT	Multi-walled carbon nanotube
N-CNT	MWCNTs from Nanocyl SA
NIR	Near infrared
PC	Performance criterion
P-CNT	MWCNTs from PlasmaChem GmbH
SDBS	Sodium dodecylbenzenesulfonate
SDS	Sodium dodecyl sulfate
SEM	Scanning electron microscopy
SWCNT	Single-walled carbon nanotube
TBOT	Tetrabutylorthotitanate
T-CNT	MWCNTs from n-Tec AS
TEOS	Tetraethoxysilane
UV	Ultraviolet
VIS	Visible light

1. Introduction

Back in the early 2000's, my father, living in a small village in China, was thinking of buying a domestic hot water (DHW) system. At that time, there was no such DHW system even in the neighboring villages. It was a big step in terms of improving living conditions for us. There were two alternative heat resources – liquefied petroleum gas and electricity. He asked me which type was safer and more economical. At that time, I was studying at a university located in southern China and I did not have any experience with DHW systems. But my wife was doing her PhD on Photovoltaics. So I suggested my father to find a solar thermal DHW system. That turned out to be a little challenge for him and finally he bought one. In the following years, solar thermal DHW system became more and more popular in the neighboring villages after my father installed an evacuated tube DHW system. After 14 years, this system is still in use with only a small decrease in efficiency. At that time, I did not know that it was just the beginning of my attraction to solar energy. After graduation, I started working in a cement factory which used coal as the only energy source for the huge energy-consuming process of limestone decomposition. The pollution was enormous and the uncertainty of safety was high. So I was wondering what would happen if we ran out of fossil fuel on earth and what a clean alternative would be. It did not take much time to find the answer on the internet – solar energy. So luckily for me, a few years later I got an opportunity to work in a solar cell factory. And here I am now really proud to present my PhD thesis about solar thermal energy which I hope will contribute to a greener application of solar energy.

Solar energy in the form of radiation from the Sun has been used since the ancient times. Today with increasing global energy demand and climate challenge, the importance of solar energy as one environmentally friendly alternative energy source has been increasingly attractive owing to its abundance, cleanliness and falling cost. Solar energy has the greatest potential amongst all renewable energy sources. The annual potential of solar energy that could be harvested on the Earth is hundredfold greater than that of the world energy demand. But currently only a small portion of the global energy consumption originates from solar energy. Since energy use for heating accounted for about half of the total world final energy consumption in 2014[1], and solar thermal technologies could also be used for

cooling and even large scale electricity production, there exists great potential for solar thermal collectors which harness solar radiation to generate heat or electricity for residential and industrial applications. Although solar thermal has been one of the most efficient methods of utilizing solar energy, the price for solar thermal systems is still high. It is therefore critical to achieve further improvements in solar thermal technologies to reduce the manufacturing cost and minimize any negative impact on the environment from the production process.

In a solar thermal collector, the key component and the most costly part, is the solar absorber, which absorbs and converts solar radiation into thermal energy. The efficiency of photothermal conversion depends on the optical properties of the absorber surface. An effective solar absorber should have a high spectral absorption in the wavelength range of the solar spectrum and a low spectral absorption in the IR wavelength region (i.e. low thermal emittance) to reduce radiative heat loss. This property is called spectral selectivity. With the development of solar thermal technology in the last few decades, various materials, design methods and manufacturing techniques have been employed to improve the spectral selectivity of solar absorbers. The photothermal conversion efficiency has been increased greatly from the original solar absorbers that used non-selective black paint surface [2, 3] to those using highly selective surfaces such as black chromium [4, 5], black nickel [6, 7] and cermet [8, 9, 10]. Among the design methods, surface texturing, tandem structure and quantum size effects have been used [11, 12]. Various thin film deposition methods like chemical vapor deposition, sputtering, electroplating, spray pyrolysis, anodization and sol-gel have been utilized to fabricate spectrally selective surfaces [13, 14].

Commercialized spectrally selective high performance solar absorbers have been available on the market for more than 20 years. However, solar absorbers using the low conversion efficiency black paints are still being sold worldwide due to their low manufacturing cost. For high efficiency solar thermal collectors, the price is elevated compared to black paint products, mainly because of the needed manufacturing equipment and the processing costs. In addition to producing inexpensive and competitive solar absorbers to meet the market demand, there are also needs and potential for further improvements to achieve more environmentally friendly utilization of solar energy, such as reducing the amount of toxic chemicals and heavy metals involved in the production process, reducing the energy demand during manufacturing and increasing long term durability of the product.

This thesis is concerned with research on a novel spectrally selective solar absorber using multi-walled carbon nanotube (MWCNT) coatings formed by electrophoretic deposition (EPD). The interest in the EPD technique is driven both by its simplicity and low material consumption. The coating process is also efficient and can be performed in air and under ambient pressure conditions by simple and inexpensive equipment [15, 16]. CNTs are known for their extraordinary electrical and mechanical properties and thermal conductivity. In this work the potential of their optical properties was explored. Since the cross sectional dimensions of CNTs are only tens of nanometers in diameter, CNTs exhibit plasmon resonance which enhances the absorption of solar radiation. In addition, with the recently introduced manufacturing methods and increasing applications of CNTs, the price has been decreasing significantly over the last decade. The research of this thesis hopefully contributes a more environmentally friendly manufacturing method for spectrally selective absorber surfaces with low chemical consumption and potentially low production cost for the solar thermal industry.

The project addresses the entire process experimentally, from the preparation of stable aqueous MWCNT suspension and the fabrication of MWCNT coating, to the protective film on top of MWCNT absorber to the final accelerated aging tests. Zeta potential measurements were performed to evaluate the stability of aqueous MWCNT suspensions. The MWCNT absorbers were characterized primarily with the use of Spectroscopy, Profilometry, and Scanning Electron Microscopy.

2. Spectrally selective solar absorbers

Solar thermal absorbers absorb and convert solar radiation into heat in solar thermal collectors. In order to be optically and thermally efficient, solar absorbers need to be spectrally selective, with a high solar absorption in the UV-VIS-NIR solar spectrum and a low thermal emittance in the IR wavelength region. Most solar absorbers are of the tandem type and consist of a IR reflective metal plate with good thermal conductivity such as aluminum [14, 17, 18] or copper [19]. On top of the metal plate, an absorbing layer is coated or fabricated which should absorb the radiation in the UV-VIS-NIR solar spectrum and be transparent to longer wavelength radiation. The transmitted longer wavelength irradiation is reflected by the metal plate. This optical combination gives a good spectral selectivity over the solar and infrared spectrum.

This chapter provides a physical background for understanding the concept of spectral selectivity in solar thermal absorbers. Since the spectral selectivity cannot be quantified directly, a description on how it is evaluated and calculated is presented.

Finally, the different designs that are capable of realizing the desired spectral selectivity in solar absorbers such as intrinsic absorbers, textured surfaces and tandem structures are briefly introduced.

2.1 Solar and thermal radiation

All materials above the absolute zero temperature emit energy in the form of electromagnetic radiation, which refers to thermal radiation. The amount of energy emitted as thermal radiation by a blackbody depends on its absolute temperature *T* and is described by Planck's law [20].

$$B_\lambda = 2hc^2\lambda^{-5}\left[e^{\frac{hc}{\lambda k_B T}} - 1\right]^{-1} \qquad \text{Eq. (1)}$$

where h is Planck's constant, c is the speed of light in vacuum, λ is wavelength and k_B is Boltzmann's constant. The symbol B_λ represents the spectral radiance measured in terms of the power emitted per unit area of a blackbody surface per unit time per unit wavelength interval.

The Sun has a surface temperature of about 5800 K [21] and continuously emits the electromagnetic radiation in a wide range of wavelengths, spanning ultraviolet visible light and far infrared. Before reaching the Earth's surface, solar radiation is absorbed by atomic molecular oxygen, ozone and nitrogen in the atmosphere. The solar radiation received at the Earth's surface spans the range from 0.3 to 1000 μm [22]. Within the range from 0.3 to 3 μm the measured radiation accounts for 98.5% of the total solar irradiance received by the Earth surface [23]. The maximum intensity is found at around 0.55 μm. This information is essential when designing solar absorbers which are intended to absorb the solar radiation as much as possible.

Fig. 1 illustrates the normalized solar irradiation distributed over the solar spectrum and the normalized thermal radiation emitted by a blackbody at the temperatures 100 ℃, 200 ℃, 300 ℃. The operation temperature of solar absorbers for household solar thermal collectors is normally less than 300 ℃ [24].

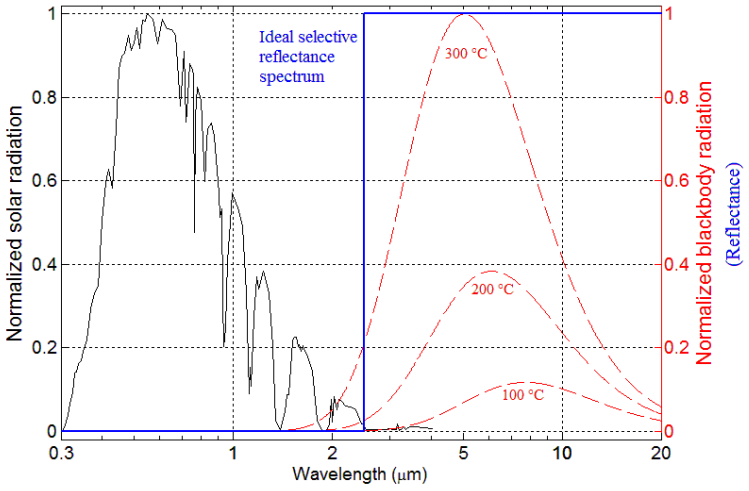

Fig. 1 The normalized solar irradiation, blackbody radiation spectra at 100 ℃, 200 ℃, 300 ℃, dashed curves. The ideal selective reflectance spectrum is indicated.

2.2 Optical characterization of solar absorbers

When incident radiation strikes a solar absorber surface, a part is reflected at the surface, absorbed in the absorber or transmitted through the absorber. The sum of reflectance, absorptance and transmittance equals 1, which can be described by Equation (2):

$$R(\lambda) + A(\lambda) + T(\lambda) = 1 \qquad \text{Eq. (2)}$$

where $R(\lambda)$is the spectral reflectance of incident radiation, $A(\lambda)$ is the spectral absorbance and is $T(\lambda)$ the transmittance. According to Kirchoff's law, for a blackbody in thermodynamic equilibrium, the absorbed energy equals the emitted thermal radiation, which is characterized by the emittance (λ) :

$$e(\lambda) = A(\lambda) \qquad \text{Eq. (3)}$$

Because of the opaque metal substrate used in solar absorbers, the transmittance is equal to zero. By substituting Equation (2) in Equation (3), Equation (4) is obtained:

$$e(\lambda) = 1 - R(\lambda) \qquad \text{Eq. (4)}$$

Solar absorbers are usually characterized by two parameters – the solar absorptance and the thermal emittance under normal incidence of radiation. Normal solar absorptance, α, is defined as a weighted fraction of the absorbed radiation to the incoming solar radiation on a surface (Equation (5)).

$$\alpha = \frac{\int_{0.3}^{2.5} I_{sol}(\lambda)(1-R(\lambda))d\lambda}{\int_{0.3}^{2.5} I_{sol}(\lambda)d\lambda} \qquad \text{Eq. (5)}$$

where the spectral solar irradiance, I_{sol}, is defined according to ISO standard 9845-1 (1992) for air mass of 1.5 [23]. λ is the wavelength of incident radiation in units of μm.

Normal thermal emittance, ε, is the ratio of emitted thermal radiation of a surface to that of Plank's blackbody, I_p, at 100 ℃ and can be calculated using Equation (6):

$$\varepsilon = \frac{\int_{2.0}^{50} I_p(\lambda)(1-R(\lambda))d\lambda}{\int_{2.0}^{50} I_p(\lambda)d\lambda} \qquad \text{Eq. (6)}$$

Wavelength ranges of 0.3 -- 2.5 μm and 2.0 -- 50 μm for evaluating solar absorptance and thermal emittance respectively are recommended by the international standard ISO 22975-3 (2014): Absorber surface durability [25]. Based on Equation (5) and (6), solar absorptance and thermal emittance can be derived from reflectance measurements.

2.3 Spectral selectivity

An effective solar absorber should have a high solar absorptance, and a low thermal emittance. That translates to a low reflectance in the wavelength range of 0.3 μm to 2.5 μm and a high reflectance in the infrared region of 2.0 μm and 50 μm. Consequently, the transition from low to high reflectance should be located between 2.0 μm and 2.5 μm for optimized solar absorbers. This optical property of solar absorbers is named spectral selectivity. An ideal solar absorber should have a solar absorptance of 1 and a thermal emittance of 0. The reflectance of an ideal solar absorber is illustrated in Fig. 1.

There are several ways to evaluate the spectral selectivity. One of the most frequently used methods is to calculate the ratio of solar absorptance to thermal emittance (α/ε). However, this method is considered to be inappropriate for the assessment of photothermal conversion efficiency. For example, a solar absorber with a solar absorptance of 0.60 and a thermal emittance of 0.03 achieves a ratio of 20 but does not have higher photothermal conversion efficiency than an absorber with a solar absorptance of 0.90 and a thermal emittance of 0.1 which achieves a ratio of only 9. The opposite is actually true since the solar absorptance is approximately twice as important as the thermal emittance. In order to rate the spectral selectivity and hence the performance of a solar absorber the expression $\alpha - 0.5 \times \varepsilon$ is instead used to reflect the weight factor of thermal emittance in a more reasonable manner. The expression was first recommended by a report of IEA solar heating and cooling program Task 27 [26], which has been employed by ISO 22975-3 [25]. In the following chapters, spectral selectivity assessed by this

expression will be employed as the main criterion for comparing the performance of prepared samples.

2.4 Different designs of spectral selective surface

To achieve the desired property of spectral selectivity, various design methods and materials have been employed for fabricating solar thermal absorbers. From a structural point of view, the methods of obtaining spectral selectivity can be classified in three categories: intrinsic selectivity, textured surfaces and tandem structures. In this section, all of these selective absorber types are introduced with most focus on tandem absorbers since they are most common commercialized products.

2.4.1 Intrinsic selectivity

Single materials which have intrinsic optical properties that are absorptive in the solar spectrum and reflective in the far-infrared region are identified as intrinsic solar absorbers. They are considered to be more structurally stable over long-term operation. On the other hand, they are less optically effective than other types of spectral selective absorbers because of either low solar absorptance or high thermal emittance, i.e. low spectral selectivity. Intrinsic solar selective materials are found in transition metals and semiconductors. Besides being used as intrinsic solar absorbers, these selective materials can also be used as a component in other types of spectrally selective absorbers [27].

2.4.2 Textured surfaces

Surface roughness or specially textured surfaces could enhance the solar absorption through optical trapping effects. When incident radiation strikes on these rough or textured surfaces, the radiation with shorter wavelengths is either immediately absorbed or scattered by the surface. The scattering leads to multiple reflections that can result in increased absorption. Simultaneously, the radiation with longer wavelength passes through the rough or textured surface and is not absorbed, instead reflected to the surroundings via multiple reflections. This type of selective absorber is less sensitive to environmental effects such as oxidation or thermal shocks and therefore has a long lifetime [12]. To achieve a high spectral selectivity,

elaborate fabrication of the textured surface is often employed. Well-known examples include textured copper and stainless steel surfaces [28, 29].

2.4.3 Tandem solar absorbers

Absorbers constructed with one or multiple layers of solar absorbing thin films coated on top of an infrared reflective metal substrate are referred to as tandem solar absorbers. The top absorbing layers are designed and coated by various methods to absorb the solar radiation while the metal substrate should reflect infrared light to reduce heat loss. Black chromium [30, 31, 32], cermet (a composite of ceramic and metal) -- for example copper oxide [33, 34, 35], cobalt oxide[36, 37, 38]), metal/oxides composites [14, 39] and spinels [40] are among the most used materials for a single absorbing layer. There are also reports on using aligned CNTs grown on metal substrates [41, 42]. As mentioned above, highly reflective metals such as aluminum and copper are commonly used as substrates. With these materials, a solar absorptance of > 0.80 and a thermal emittance of < 0.2 can readily be achieved.

In order to improve solar absorption and increase the spectral selectivity of solar absorbers, a tandem structure of multi-layered thin films deposited on reflective metal substrates is also often used. The multi-layered thin films acting as interference stacks usually consist of at least one dielectric layer and one anti-reflection layer. By using destructive interference, reflectance is minimized in the solar spectrum and the overall solar absorption can be increased.

Inverse tandem structures are another alternative for achieving spectral selectivity. It is usually realized by laying an infrared reflective layer on the top of an absorbing material. The top layer is transparent in the short wavelength region and allows the solar irradiation to be absorbed by the underlying absorbing material. Indium tin oxide (ITO) deposited on top of silicon is one of the examples. ITO is a well-known transparent thin film in the visible light range. The underlying silicon acts as the absorbing material. However, silicon is an inferior solar absorber and the overall efficiency of this inverse tandem structure is poor.

The tandem structure of solar absorbers can be constructed by various processes. In this work, the tandem structure is fabricated by electrophoretically depositing a CNT coating on an aluminum substrate.

3. Optics of thin films

This chapter gives a fundamental physical background for understanding how electromagnetic radiation interacts with matter. An introduction on the enhanced absorption of nanoparticles is also presented.

3.1 Electromagnetic radiation and absorption

The behavior of electromagnetic radiation interacting with matter alters qualitatively as its frequency changes. When a plane electromagnetic wave propagates in an absorbing medium with a complex refractive index N = $n + ik$, where n is the real part of the refractive index and k is the imaginary part (also called the extinction coefficient), its electric field in the x-axis can be expressed as [43]:

$$E(x,t) = E_0 \exp(-k\omega x/c + i(n\omega x/c - \omega t)) \qquad \text{Eq. (7)}$$

where E_0 is the initial amplitude of electric field; $E(x,t)$ is the amplitude of electric field at the time t and the position x; ω is the angular frequency and c is the speed of light in vacuum. Equation (7) indicates that the amplitude attenuates in the direction of propagation in the medium, and the optical constants (n and k) are of great importance for the attenuation. And according to Beer-Lambert law, the attenuation of light is correlated to the absorption coefficient α and the propagation distance, x:

$$I = I_0\, exp(-\alpha x) \qquad \text{Eq. (8)}$$

where I is the change in light intensity; I_0 is the initial intensity before the electromagnetic wave entering the medium, and the light intensity I is proportional to the square of amplitude:

$$I \propto E(x,t)^2 = E_0^2\, exp(-2\omega k x/c) \qquad \text{Eq. (9)}$$

Combining equations (8) and (9), the correlation between α and k is derived:

$$\alpha = 2\omega k/c = 4\pi k/\lambda \qquad \text{Eq. (10)}$$

where λ is the wavelength of light. When a light passes through an absorbing thin film with a thickness of d, an expression for the change of intensity can be obtained by combining equation (8) and (10):

$$\ln\left(\frac{I}{I_0}\right) = -\alpha x = -\alpha d = -4\pi\frac{kd}{\lambda} \qquad \text{Eq. (11)}$$

Equation (11) is very important for designing a spectrally selective surface. It indicates that two variable parameters k and d can be modified to control the spectral selectivity. k is determined by the applied material of the thin film, which could be a single material or a composite (for example, cermet). If the film is too thin i.e. $\lambda >> kd$, it becomes transparent. If the film is too thick, light with longer wavelengths is also absorbed.

3.2 Absorber performance enhancing methods

Even a well-designed spectrally selective absorber will still exhibit some undesired reflection which leads to reduced solar absorptance. Several methods could be used to suppress this undesired reflection to improve the overall absorption, such as anti-reflection (AR) coating and multilayers with graded refractive indexes.

3.2.1 Anti-reflection optics

The purpose of AR coating is to create double interfaces – the interface between the surrounding and the AR coating, and the interface between the AR coating and the underlying layer. By choosing an appropriate thickness and refractive index of the AR coating, destructive interference between reflected light from the upper and lower interface of the AR layer can be created, i.e., light reflected at the upper interface will be out of phase with light reflected from the lower interface. Hence the reflectance at a desired wavelength could be reduced theoretically to zero. However, this is actually only true for non-absorptive materials, i.e. when k is

equal to zero. In order to achieve this effect, the thickness *d* of the AR coating with a real part of the refractive index n_1 should be designed as:

$$d = \lambda/4n_1 \qquad \text{Eq. (12)}$$

where λ is the wavelength at which the minimum reflectance is desired. And the optimal refractive index n_1 should be identical to the geometric mean of the surrounding and the underlying layer. This can be expressed by:

$$n_1 = \sqrt{n_0 n_2} \qquad \text{Eq. (13)}$$

Dielectric materials are commonly used as AR coatings, such as magnesium fluoride (MgF_2) and silica (SiO_2) owing to their transparence over a wider wavelength range and low refractive index. The *n* value at 550 nm is 1.38 for MgF_2 [44], and 1.46 for SiO_2 [45]. For the cases requiring an even lower refractive index of the AR coating, nanoporous materials can be a good option. However, surface treatments or the addition of a cover layer on top of nanoporous materials is usually needed to protect the nanoporous layer or maintain the anti-reflection effect.

3.2.2 Graded refractive index

While a single layer AR coating can create a reflectance minimum at one desired wavelength, multiple absorber and AR coatings in a stack with elaborately designed graded refractive index could minimize the reflectance in a wider range of wavelengths, hence solar absorption is greatly enhanced. Many methods have been developed to model the multilayer design [46, 47].

3.3 Absorption of nanoparticles

Particles of sizes between 1 and 100 nm are categorized as nanoparticles. It is well-known that the significant increase in surface area of nanoparticles results in unexpected mechanical, electrical and optical properties compared to what their bulk materials exhibit. Owing to the strong plasmon resonance and consequent strong absorption of electromagnetic radiation in the visible and near-infrared spectral range [48], they are good candidates as solar absorber materials. High

spectral selectivity with a high solar absorption in the visible range while maintaining a low infrared emission can be realized using nanoparticles as an absorbing layer [49].

Carbon nanotubes in essence have a high anisotropy with a diameter from a few to dozens of nanometers and a length up to micrometers. Their plasmon excitations have been studied by Thomas Stöckli and his colleagues using Electron-energy-loss spectroscopy (EELS) [50].

4. Methodology

This chapter outlines the methodologies employed in this work. Firstly, the method used for computational simulation of carbonaceous spectrally selective absorbers is described. Thereafter, the characterization tools and the determination method of optical constants of MWCNT coatings are presented. Finally, the procedure employed to perform accelerated ageing tests on MWCNT absorbers is explained.

4.1 Simulation of solar absorbers

Carbonaceous materials have attracted increasing research attention as solar absorbing materials [51,52] owing to their abundance in nature and suitable properties such as high absorption over the solar spectrum and stability against heat, water and chemicals. Computational simulation of spectrally selective absorber using monolithic carbonaceous materials as absorbing layer on aluminum substrate was performed using the Setfos 3.4 software from FLUXiM [53]. The carbonaceous materials studied included graphite, soot and single-walled carbon nanotubes (SWCNT). The carbon-based absorbers were also simulated with a top coating of a dielectric such as alumina or silica functioning as an anti-reflection (AR) layer.

4.1.1 Simulation of absorbing layers

The simulated absorbers consisted of an absorbing layer on the top and a 0.5mm thick aluminum plate as the substrate. A 10 nm interlayer of alumina caused by natural oxidation was inserted. Absorbing carbonaceous materials included graphite, soot and SWCNT. The optical constants for these materials were found in reference literature [54, 55, 56, 57] and imported into Setfos. Various thicknesses of each type of absorbing layer were simulated and the resulting spectral reflectance in the wavelength range from 0.3 to 20 μm was calculated. Note that no refractive indices at wavelengths longer than 0.9 μm were found for SWCNT. Setfos in this case takes the refractive index values at 0.9 μm and keeps them constant all the way to 20 μm. This assumption could have an impact on the thermal emittance of SWCNT absorbers. However, the solar absorptance values are considered to be acceptably accurate for the purpose of this study.

4.1.2 Simulation of absorbers with anti-reflection layer

The spectral selectivity could be enhanced by depositing an anti-reflection layer on top of the solar absorbers. Their refractive indices were taken from the database of Setfos 3.4 and were only available up to 1.7 μm on wavelength, then treated as constant up to 20 μm. This approximation could affect the accuracy of the prediction. For example undesired absorption in the IR could be missed. However, experimental results have showed that the thermal emittance of alumina and silica AR coatings coated solar absorbers does not increase, provided they are thinner than 100 nm [24]. To find the optimal thickness of an AR layer, the simulations were carried out with a step size of 10 nm from a starting thickness of 10 nm.

4.2 Refractive index determination

The optical properties of CNTs depend on the diameter of tubes, the structure (chirality), production methods amongst other properties [58, 59, 60]. In addition, the coating process will also affect the optical properties, for example, the coating composition, the formation status of CNT (standing vertical, parallel to substrates or angled in between) and CNT fractional composition. Therefore, it is not realistic to expect to find optical constants available in the literature that matches the MWCNT coatings prepared in this study.

Spectroscopic Elliopsometry is a powerful tool for characterization of thin films by measuring the change in polarization upon reflection or transmission of incident light after interacting with the thin films being investigated [61]. An M-2000 spectroscopic ellipsometer configured with automated angle from J.A. Woollam Co. was used to determine the complex refractive index of MWCNT coatings.

4.3 Characterization tools

4.3.1 Optical characterization

The normal total (diffuse and direct) spectral reflectance of all the prepared absorber samples was measured in the wavelength interval 0.3-20 μm. A Perkin-Elmer Lambda 900 spectrophotometer was employed in the 0.3-2.5 μm wavelength range. It was equipped with an integrating sphere of 150 mm diameter, circular beam entrance and sample port of 25 mm. A spectralon sample was used for

reference. Normal total spectral reflectance in the infrared wavelength range 2.0-20 μm was measured by a Bruker Tensor II FT-IR spectrophotometer. A mercury cadmium telluride detector was cooled by liquid nitrogen for the IR measurements. The reflectance data obtained was used to calculate normal solar absorptance α and normal thermal emittance ε of solar absorbers as outlined in section 2.2. It is worth noting that an extrapolation method was introduced to estimate the reflectance from 20 to 50 μm so that the calculation of ε (see Eq. (6)) can be completed. The standard deviation of α and ε was respectively 0.002 and 0.02, calculated from repeated reflectance measurements of the same sample over an extended time period.

4.3.2 Morphology: Scanning electron microscopy

A ZEISS Merlin VP Scanning Electron Microscope (SEM) with a field emission gun and a high resolution of 0.8 nm/15 kV was used to examine surface morphologies of different MWCNT coatings, absorber samples after accelerated ageing tests, and protective films. The images were produced at an accelerating voltage of 15 kV.

The coating thickness and surface roughness were examined by Veeco NT9080 Profilometer which uses high precision white light interferometry to analyze height differences and variation. The measurement area was 94 μm x 125 μm. 5% cursor width representing a width of 6.3 μm was used when analyzing the surface roughness.

4.3.3 Atomic composition

An Energy Dispersive X-ray detector equipped to the ZEISS Merlin VP SEM was used for elemental analysis.

4.4 Accelerated ageing tests

Compared to the optimization of the spectral selectivity of solar absorbers, their long-term durability has not received enough concerns. The international standard for absorber surface durability was only issued 2 years ago. Included in the thesis work, the performance degradation due to ageing of the investigated MWCNT solar absorbers was examined.

During the operation of solar collectors, the solar absorber surface is exposed to various external environmental effects, such as condensed water, high temperature and airborne pollutants. These could cause deterioration to the surface of absorbers. For instance, elevated temperature combined with condensation during the operation could accelerate different kinds of chemical reactions, which leads to a higher rate of material degradation and consequently the performance. At high temperatures, the oxidization of the thin film absorber and/or the substrate surface is promoted, possibly resulting in the loss of spectral selectivity. Hence, the impact caused by long term exposure to the external environment needs to be studied in order to evaluate the life-time performance of solar absorbers. The most accurate way is to assess it under normal operation conditions. However, in order to reduce the testing time, accelerated ageing tests in a short period in laboratories are usually performed.

In this study, accelerated ageing tests followed the recommendations of the international standard ISO 22975 solar energy – collector components and materials – Part 3: Absorber surface durability [25]. The tests include condensation test, thermal stability and high humidity air containing sulfur dioxide test. For the MWCNT absorbers studied in this work, the target application is for flat-plate solar collectors. In this case, only the first two tests are critical and therefore the third was not carried out.

4.4.1 Equipment

A climate chamber VCL 4010 from Vötsch Industrietechnik was used to perform the condensation test. The temperature and the relative humidity in the inner chamber can be controlled in the ranges of 10~95 °C and 10~98%, respectively. In order to create condensed water on samples, a lower temperature than the setting value in the chamber was maintained by a circulating water pipe, which was connected to a thermoregulator Techne TE-10D Tempette, running through the sample holder.

The accelerated thermal stability test was performed using a tube furnace Entech, ESTF 40-120/11.

4.4.2 Testing procedures

Both the condensation tests and the thermal stability tests were carried out in specified test intervals of 150, 300 and 600 hours. In all the tests, always two samples with each protective film coated absorber were tested in order to obtain an indication of the variability of the results.

As specified by the standard procedure for the condensation test, the temperature and humidity in the inner chamber were set to 45 ℃ and 95% respectively for all samples. The circulating water through the sample holder from the thermoregulator had a temperature of 40 ℃ so that condensation of water on the surface of the tested samples was ensured. During the entire test, condensation droplets of water could be observed on the sample surface at all times. After specified test intervals, the samples were taken out of the climate chamber and dried at ambient conditions (room temperature around 20 ℃ and relative humidity of 30~60%) before reflectance measurement for the assessment of durability.

For the thermal stability test, ISO 22975-3 suggests test temperatures based on optical properties i.e. solar absorptance and thermal emittance and the corresponding maximum operating temperature $T_{\max}$. For the MWCNT absorbers investigated in this work, $T_{\max}$ is between 186-190 ℃, and the corresponding recommended test temperature is 259 ℃. A slightly higher temperature of 265 ℃ was used for all the samples in this work. Samples were placed in the tube before the oven temperature was ramped up at a rate of 50 ℃ per minute. The temperature was then kept constant at 265 ℃ until the end of each test. After that, heating was turned off and the tested samples were kept in the oven until the temperature had decreased to 100 ℃. Then the samples were moved out for faster cooling to room temperature. Reflectance measurements were then performed for the assessment of durability.

The durability of the absorber surface was assessed by the following performance criterion (PC):

$$\mathrm{PC} = -\Delta\alpha + 0.5\Delta\varepsilon$$

where $\Delta\alpha$ is the change in solar absorptance and $\Delta\varepsilon$ is the change in thermal emittance after testing. The 0.5 factor reflects the lesser importance of a change in

thermal emittance compared to a change in solar absorptance. In this study, the qualification procedure was:

- If PC > 0.015 after 150 hours of testing, the absorber surface is disqualified;
- If PC ≤ 0.015 after 600 hours of testing, then it is qualified.

The threshold value of 0.015 means that the optical performance of absorber surface during the service life time is expected to reduce to no more than 98.5% of its original value. It is based on a design service life time of 25 years. It is worth noting that a negative PC value would indicate a factual improvement of the spectral selectivity over service life-time. The following diagram (Fig. 2) indicates the qualification scheme described above.

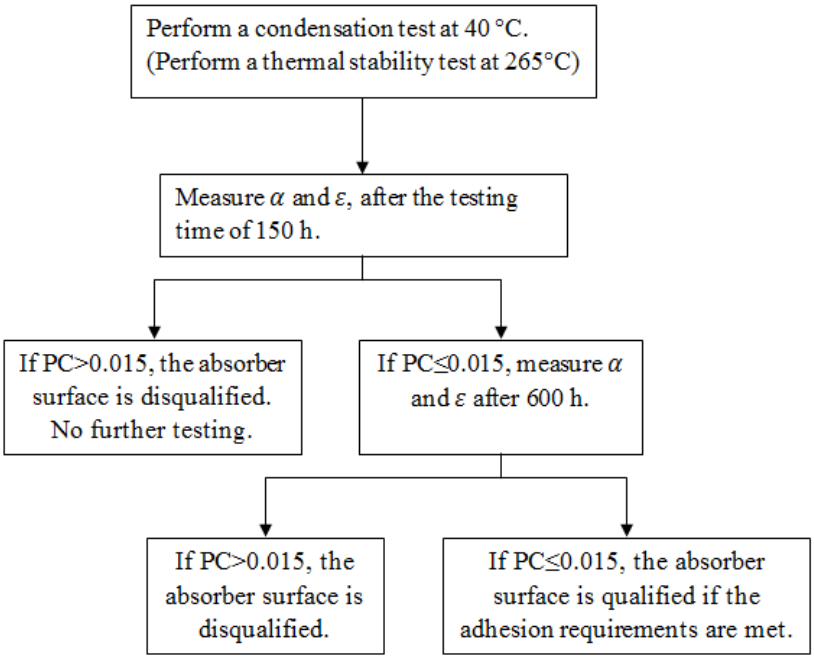

Fig. 2 Qualification scheme for condensation test and thermal stability test

The used qualification procedure in this work is slightly different from the standard. In ISO 22975-3 there is also a possibility for an absorber to be qualified even though the PC value is > 0.015 after 600 hours of testing. However, this possibility has been removed in this work and Fig. 2 in order to make the testing simpler and even stricter.

5. Sample preparation

The solar absorber was fabricated by electrophoretically depositing a multi-walled carbon nanotube (MWCNT) coating on an aluminum substrate. Kinetically stable aqueous CNT suspensions were prepared and used for the electrophoretic deposition. Heat treatment was performed to solidify the MWCNT coating [62]. Thereafter, an anti-reflective and protective thin film was spin-coated on top of the MWCNT coating using various sol-gel solutions, like silica, hybrid silica and silica-titania. The AR thin films were then subjected to heat treatment before optical characterization and other tests were performed on the finished MWCNT absorbers [63]. Deionized (DI) water used in this study had a resistivity > 5 MΩ·cm and was produced using the process of reverse osmosis by a Septron Line 10 Pro from Christ Aqua AB.

5.1 Aluminum substrates

To achieve high spectral selectivity, the absorber substrates should have high reflectivity in the infrared region so that the heat loss via infrared emission is minimized. Specularly reflecting pure aluminum (Al) plate from Metallvaruhuset Sverige AB was used as the substrate for the MWCNT absorbers. The as-received Al plate, which was covered with a layer of blue plastic film to protect the specular surface from scratches and damage, had a surface roughness R_q (root mean squared) of 0.04 μm. Due to exposure to air, there is a very thin layer (<10 nm [64]) of alumina on the top of surface. The Al plate was cut to substrate pieces with a size of 32 mm x 30 mm.

The conductivity of alumina is lower than that of aluminum, which affects the electrophoretic deposition, therefore an etching process was performed to remove the alumina on the top of Al substrates. The etching solution was prepared by mixing 1 l deionized (DI) water, 35 g of CrO_3 power and 20 ml of 85% phosphoric acid. The Al substrates were etched for 8 minutes in heated (80 °C) etching solution. Then the etched substrates were rinsed in water and dried by blowing with nitrogen [24]. EPD experiments were also performed on un-etched Al substrates to investigate the influence of the pre-treatment on the final MWCNT coating result.

5.2 Suspension of Carbon nanotubes

Carbon nanotube (CNT) is a needle-like tube structure of carbon. It was firstly observed and synthesized by Ijima in 1991 [65]. CNTs are usually classified as single-walled (SWCNT) or multi-walled (MWCNT). CNT structure can be imagined as a rolled up graphene sheet for SWCNT, or as rolled-up layers of multiple graphene sheets for MWCNT [66]. CNTs have a diameter in the nanoscale and a length up to micro meters. Over the last decades, they have attracted considerable attention due to their unique atomic structure, outstanding mechanical, electrical and thermal properties [67, 68, 69, 70, 71, 72]. Extensive scientific and technological studies on their potential applications have been conducted in many fields including sensing [73, 74], electronic devices [75, 76], biomedical products [77, 78], structural composites [79, 80] , Hydrogen storage [81, 82], thermal management [83, 84], and catalyst supports [85, 86]. CNTs are expected to substitute for a variety of conventional materials in the near future [87].

Besides the attractive properties, the toxicity of airborne fine CNTs in particle form has to be addressed. Airborne fine CNTs can induce harmful effects as inflammatory and fibrotic reactions if they reach inner organs [88, 89], however other studies indicated that the environmental risk is low compared to other common industrial manufacturing process [90]. In this work, the CNTs are mixed with water and surfactants and can consequently not be inhaled. However, care has to be taken when mixing the CNT powder with the other ingredients.

To allow the manipulation and exploration of potential applications of CNTs, it is often a requirement that CNTs are dispersed uniformly in organic solvents or aqueous solutions. However, as-produced CNTs are intrinsically inert, extremely hydrophobic and tend to aggregate due to the strong Van der Waals interaction forces along the length axis [91, 92]. Their hydrophobic nature limits the dispersibility in most solvents, which becomes a technical barrier for many applications that require homogeneous dispersion of materials. In the scope of this work, the development of a more environmentally-friendly process for fabricating solar absorbers was one of the main objectives. Therefore, utilizing aqueous MWCNT suspensions was deemed essential for the coating deposition.

5.2.1 Stabilization methods of MWCNT suspension

When as-produced MWCNTs are added to aqueous solution, a stable colloid suspension is not spontaneous formed. The individual tubes exfoliated from CNT aggregates by external energy are unstable and prone to re-aggregate due to Van der Waals force [93, 94], unless a dispersion agent is present. The dispersion agents used for the stabilization of CNTs in aqueous solutions can be classified as surfactants and polymers.

The molecules of surfactants usually consist of two groups – a hydrocarbon chain (hydrophobic tail) and a polar group (hydrophilic head). The polar group may be ionic or nonionic. The ionic group can be anionic or cationic [95]. When surfactant is added to an aqueous solution containing CNTs, with the help of agitation, stabilization is achieved due to the adsorption of the hydrophobic tails of the surfactant molecules on the nanotube surface while the hydrophilic head groups are oriented toward the aqueous phase. This absorption forms an energy barrier created by electrostatic repulsion that prevents the re-aggregation of CNTs [96, 97].

Polymers can be physically adsorbed onto the surface of CNTs and prevent CNT surfaces coming into close contact. The resulting steric repulsion enhances the dispersion of CNTs and stabilizes the colloidal suspension [98, 99]. However in some cases, the polymer is undesirable and could be difficult to remove.

Although the preparation of kinetically stable aqueous MWCNT suspensions has been extensively reported, there are also many contrary results published. There are many factors that affect the dispersion of CNTs in aqueous solution, including the synthesis methods, number of walls (single, double or multi) and functionalization of CNTs, surfactant types, surfactant concentration, external energy sources and pH values. A successful recipe for preparing a stable aqueous CNT suspension is system dependent and requires extensive experimental trials.

5.2.2 Preparation of aqueous MWCNT suspensions

Three types of MWCNTs were investigated: T-CNT, N-CNT and P-CNT. Aqueous T-CNT suspension was provided by the company n-Tec AS and consisted of functionalized MWCNTs, DI-water and an anionic surfactant. The T-CNT suspension had a solid concentration of 1 g/l and was stable for months. It was subjected to a sonication bath for 2 hours before the deposition process. P-CNT and

N-CNT were also functionalized MWCNTs and obtained from the companies PlasmaChem GmbH and Nanocyl SA, respectively. These two types of as-purchased MWCNTs were used to prepare aqueous MWCNT suspensions without any additional pre-treatments.

Three different ionic surfactants -- sodium dodecyl sulfate (SDS), sodium dodecylbenzenesulfonate (SDBS) and Hexadecyltrimethylammonium bromide (CTAB) were tested for the stabilization of N-CNT and P-CNT in aqueous solution. SDS and SDBS are anionic surfactants while CTAB is a cationic type. These surfactants are non-toxic for humans and are widely used in cleaning, hygiene, laundry detergent and hair conditioning products. SDS, SDBS and CTAB are also highly biodegradable [100, 101, 102]. All of them have been previously studied as dispersing agents for CNTs [103, 104, 105]. They were purchased from Sigma-Aldrich and used as-received.

To prepare aqueous N-CNT and P-CNT suspensions, a certain amount of each surfactant was firstly dissolved in DI water with assistance of stirring before adding N-CNT or P-CNT. Then the mixtures were subjected to agitation in a sonication bath for 24 hours in order to disperse MWCNTs completely in the aqueous solution. Both of the obtained suspensions had a solid content of 0.1wt% and the concentration of SDS, SDBS and CTAB were 0.25%, 0.2% and 0.25%, respectively. The kinetically stable suspensions can be stored for months with insignificant sedimentation.

5.2.3 Stability evaluation of aqueous MWCNT suspension

Various characterization tools have been employed for evaluating the dispersion state of MWCNTs in aqueous suspensions, for example, Zeta potential[106, 107], UV-Vis or NIR Spectroscopy [108, 109, 110], surface tension[111], Transmission electron microscopy (TEM) [112] and Raman and Fluorescence Spectroscopy [113]. During the preparation work in this study, the stability of aqueous MWCNT suspensions was examined by the amount of sediment, and by quantitatively measuring the Zeta potential (ζ).

Surface charge induced by ionic surfactants results in electrostatic repulsion among individual MWCNTs, which enhances the stability of the MWCNT suspension. MWCNTs at the kinetically stable state have an electrophoretic mobility that can

be measured, and the mobility can be used to calculate Zeta potential for a given system. Zeta potential is proportional to the electrostatic repulsion force between charged CNTs. Therefore it is a measure of stability. An increase of Zeta potentials enhances electrostatic stabilization. With a Zeta potential close to zero, electrostatic repulsion becomes small compared to the existing Van der Waals attraction. The low Zeta potential eventually can result in aggregation followed by sedimentation and phase separation [95].

Zeta potential of the aqueous MWCNT suspensions were measured by a Zetasizer Nano Z system (Malvern Instruments, UK) using Laser Doppler Micro-Electrophoresis.

5.3 Electrophoretic deposition

Surfactant suspended MWCNTs are surface charged due to the absorption of cationic or anionic group. The surface charged MWCNTs exhibit electrophoretic motion, moving towards the electrode with the opposite charge under an applied electric field. Thereafter, MWCNTs are accumulated at the electrode and form the deposit [114]. Cationic surfactants give a positive charge to MWCNT surface resulting in a deposition at the cathode while anionic surfactants lead to deposition at the anode.

A schematic diagram of the EPD set-up is shown in Fig. 3. Specularly reflecting aluminum plates were connected to a power supply and used as the electrodes and as the substrates for the solar absorbers. During the EPD process, the two aluminum substrates were immersed in an aqueous MWCNT suspension contained in a glass beaker.

Traditionally EPD is applied with direct current (DC). Water electrolysis has a standard potential of 1.23 V, at voltages above this water electrolysis occurs resulting in evolution of hydrogen at the cathode and oxygen at the anode. In some cases, the evolution of hydrogen gas and the electrode oxidation could cause inferior coating quality. Therefore alternating current (AC) EPD can be used to avoid or minimize water electrolysis. In this study, both AC and DC EPD were tested.

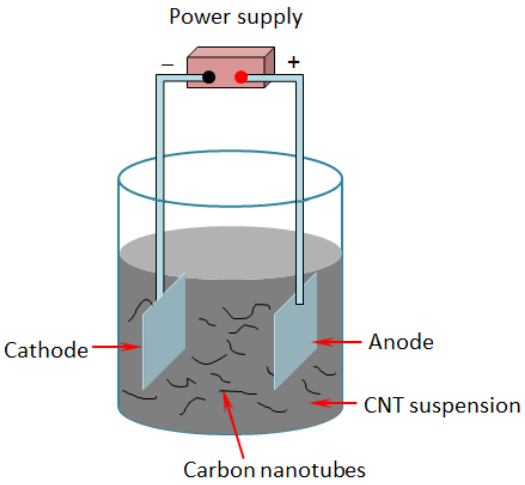

Fig. 3 schematic diagram of EPD set-up

For DC EPD, deposition mass i.e. coating thickness on planar aluminum substrates is proportional to solid concentration, electrophoretic mobility, electric field and deposition time [115]. The electric field depends on the applied voltage and the inter-electrode spacing. To achieve homogenous MWCNT coating and various coating thicknesses, the applied voltage, the inter-electrode spacing and deposition duration were tuned in the experiments. As reported in Paper III [116], there was a voltage threshold of 15 V for attaining homogenous MWCNT coating. Under lower voltages there was little deposition of MWCNTs and poor adhesion of the MWCNTs to the aluminum substrate. Therefore, the applied voltage was set to 25 V unless specified otherwise. The inter-electrode spacing was fixed to 1 or 2 cm. The deposition time was a few seconds and adjusted in order to obtain different coating thicknesses.

5.4 Anti-reflection coating

Porous silica (PS) coating were tested as AR layer for the MWCNT absorbers. A PS precursor solution was prepared using Tetraethoxysilane (TEOS, ≥99%) by the sol-gel method. Firstly, TEOS was mixed with ethanol before DI water was added. HCl was used as hydrolyzing catalyst. After stirring for half an hour, a pore-forming agent Pluoric® F127 (PF127, Sigma-Aldrich) was added to the silica sol.

Then it was allowed to hydrolyze for 2 hours before coating. The molar ratio of TEOS: EtOH: H_2O: PF127 was 1: 50: 15: 0.008.

5.5 Protective films

To improve the durability of solar absorbers, a protective layer can be added on top of the absorbing layer. This layer has to be dense enough to prevent penetration of condensed water so that the underlying metal surface is protected from oxidation or corrosion. Since the added layer could have an impact on the optical properties, it should be thin enough to avoid any increase in thermal emittance. Silica and silica-titania coatings have been employed as anti-reflection and/or self-cleaning layer/protective in many different applications [117, 118]. In this study, different silica and silica-titania formulations were tested as protective film against moisture and condensation. A previously developed sol-gel method was used to prepare silica and silica-titania solutions [24]. All the chemicals used in these experiments were from Merck and were used without pre-treatment.

5.5.1 Silica and hybrid silica films

TEOS and methyltrietoxysilane (MTES, ≥99%) were used as silica precursors. Silica films using both a single precursor (TEOS) and dual precursors (TEOS/MTES) were fabricated. The use of dual precursors results in the formation of a hybrid silica film. A higher proportion of MTES in relation to TEOS results in a more flexible film.

TEOS was firstly mixed with ethanol (≥99.5%) before DI-water containing HCl (37%) was added. HCl was used as catalyst for the hydrolysis of TEOS. The molar ratio of TEOS : EtOH : H2O : HCl was equal to 1 : 35 : 5 : 0.04. In order to hydrolyze TEOS, the resulting mixture was stirred for 2 h at room temperature before coating. For preparing hybrid silica films, the desired molar ratio of MTES was then added into the solution. The mixture was stirred in a closed container for 6 hours to ensure full hydrolysis. The obtained solutions maintained stable for weeks.

5.5.2 Silica-titania film

Two silica-titania films with different proportions of silica and titania (50/50 silica-titania and 70/30 silica-titania) were produced. Tetrabutyl orthotitanate (TBOT, ≥98%) was used as titania precursor. Firstly, TEOS, ethanol, DI-water and HCl were mixed and stirred for 30 minutes. Then the mixture was diluted with ethanol before acetylacetone (≥99%) and Tetrabutyl orthotitanate were sequentially added. The final molar ratios of TEOS : EtOH : H2O : HCl : TBOT : acetylacetone were 1 : 66 : 4 : 0.04 : 1 : 1 for 50/50 silica-titania sol and 0.7 : 30 : 4 : 0.04 : 0.3 : 0.3 for 70/30 silica-titania sol. The resulting sols were stirred for 6 hours before coating process.

5.6 Spin-coating

Silica, hybrid silica, silica-titania, and PS coatings were spin coated on top of MWCNT solar absorbers by a spin-coater, Specialty Coating Systems SCS 6800. At first, a syringe containing 0.3 ml of precursor solution was ejected onto the center of the sample surface. The solution then spread and covered the surface in a fraction of a second. A 30 sec spinning process allowed further evaporation of solvents and formation of a homogeneous coating. The spin speed was tuned between 1500 and 6000 rpm for adjusting the coating thickness. The protective film and PS layer coated MWCNT absorbers were dried for a few minutes in ambient conditions before heat treatment.

5.7 Heat treatment

After EPD and protective film coating the samples were heat treated in a tube furnace under an atmospheric environment. The heating rate was fixed at 50 ℃ per minute for all the treated samples. Peak temperature T_p and dwell time (t) at T_p were adjusted for different types of samples and purposes. Based on the reported results [116], T_p and the dwell time for the heat treatment of MWCNTs absorbers was set to 500 ℃ and 5 minutes, respectively, unless specified otherwise. T_p for the heat treatment of silica and silica-titania coatings was 400 ℃ and 500 ℃, respectively. There was no dwell time for the heat treatment of protective films. The PS coatings were dried at 80 ℃ for half an hour and heat treated at 450 ℃ for 45 minutes. The heating was turned off when the dwell time was completed for the MWCNT absorbers with and without PS coating, and when the peak temperature

T_p had been reached for protective film coated absorbers. The samples were left in the tube furnace until the temperature decreased to 300 ℃ before they were removed to room conditions for fast cooling.

6. Simulation results

The simulation results for solar absorbers using carbonaceous materials of graphite, soot and SWCNT as absorbing layers with and without anti-reflection (AR) coating have been published in *paper II* [119]. Here they are briefly introduced. For more detailed results, please refer to the paper.

6.1 Simulation of absorbing layers

For all three types of carbonaceous materials, there was an optimal thickness: 80 nm for graphite, 120 nm for soot and 430 nm for SWCNT. The suspected reason for the SWCNT layer having a notably higher optimal thickness was that the refractive index of the SWCNT material was based on SWCNTs embedded in a matrix rather than pure SWCNTs. At the optimal thickness, the achieved spectral selectivity was 0.63, 0.82 and 0.85 for graphite, soot and SWCNT respectively. The reason why soot and carbon nanotubes (CNT) are better in absorbing sunlight compared to graphite is attributed to the material composition. Soot and CNT consists of nano sized elements while graphite is a bulk material. Owing to the plasmon absorption effect, nano-particulate materials are much more efficient in absorbing sunlight than bulk materials.

6.2 Simulation of absorbers with anti-reflection coating

An AR coating is most effective when its real refractive index (n) is the square root of the real refractive index of the material that it is deposited on. At this optimal refractive index, a desired destructive interference is created to reduce the reflection. Since the maximum solar intensity is at a wavelength of 550 nm, the reflection at this point should be minimized to increase the absorptance. Commonly used AR coatings made of silica and alumina were selected for soot and graphite respectively. For SWCNT absorber, the n value of a SWCNT film at 550 nm (n=1.58) is equal to 1.26. There is no bulk material having such low refractive index. Nanoporous materials would be a good option. However, no data for materials with a refractive index covering the necessary wavelength range was

found. The best available match is silica (n=1.45 at 550 nm). Therefore, a silica film was applied in the simulation of AR layer for SWCNT absorber.

With an AR layer, the solar absorptance increased from 0.65 to 0.87 for a graphite absorber, from 0.82 to 0.91 for a soot absorber and from 0.88 to 0.91 for a SWCNT absorber. The thermal emittance remained unchanged for all the absorbers.

7. Characterization results

This chapter summarizes results from all the experiments except for the accelerated ageing tests. Some of results were used to determine parameters or methods for the subsequent experiments. For those results that have been published in the listed papers, only brief conclusions are transcribed here.

7.1 Stability evaluation of aqueous MWCNT suspensions

The stability of prepared aqueous N-CNT and P-CNT suspensions was firstly evaluated by assessing the amount of sediment. Both of the two suspensions with the SDBS surfactant were unstable. Sedimentation occurred soon after sonication was stopped. A significant amount of sediment was observed within one hour. Higher dosage of SDBS and longer sonication time did not significantly improve the dispersibility.

For CTAB assisted aqueous N-CNT and P-CNT suspensions, the amount of sedimentation was minor. The stability of these two suspensions was much better than those containing SDBS. However, CTAB as a cationic surfactant results in deposition on the cathode on which hydrogen evolution occurred due to water hydrolysis. This resulted in poor quality of MWCNT coatings and therefore this method was not pursued.

SDS assisted N-CNT and P-CNT suspensions both exhibited good stability. The measured zeta potential was -22.2 mV and -42.0 mV for N-CNT and P-CNT suspensions, respectively. The minus values indicate a negative charge of surface and therefore deposition occurs on the anode during EPD. The two aqueous suspensions were stable for months with insignificant sedimentation.

The zeta potential of T-CNT suspension provided by n-Tec was -26.1 mV, and it is stable for many months.

7.2 AC and DC EPD

For AC EPD, various waveforms, time ratio of forward/reverse voltage and voltage values were tested. Unfortunately, homogenous MWCNT coatings were not obtained. One of the reasons suspected for the poor coating quality was that the deposited MWCNTs were partly removed by the reverse voltage. Another assumption was that the adhesion of MWCNTs to the substrate was reduced, which resulting in the peeling of MWCNTs when the substrate was lifted from the MWCNT suspension. Further tests are necessary to improve the homogeneity of MWCNT coatings deposited by AC electrophoresis. Thus all the MWCNT solar absorbers were prepared using DC electrophoresis.

7.3 Effect of aluminum substrates

It has earlier been reported [24] a higher spectral selectivity on etched Al substrates compared to optically rough Al substrates using spin-coating process since advantages of thin film interference more easily can be utilized on smooth surfaces.

Only optically smooth aluminum substrates were used in this work. The reflectance spectra of the Al substrates before and after etching are shown in Fig. 4. As illustrated in the figure, the reflectance in the UV-Vis-NIR region increased after etching. This resulted in a decrease of solar absorptance from 0.16 for as-received to 0.12 for etched Al substrates, indicating a more reflective surface. The important region where the substrate should be highly reflective is in the far-infrared, and here there is no difference between as-received and etched Al substrates. For both Al substrates, the reflectance in the far-infrared region was over 95% and the thermal emittance was 0.06.

The roughness measurement indicated an even smoother surface after etching, with the root mean square roughness changing from 0.04 μm for as-received Al substrates to 0.01-0.02 μm for etched surfaces.

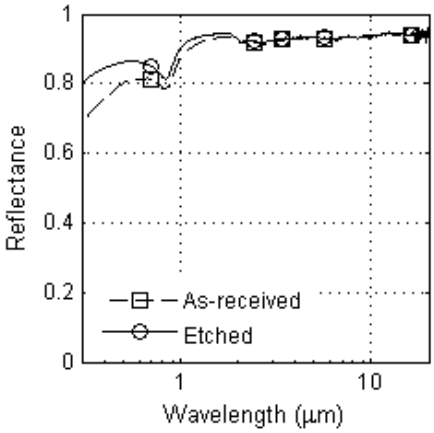

Fig. 4 Reflectance spectra of Al substrate before (dashed curves) and after (solid curves) etching.

However, the etching process was found to be undesirable for EPD of MWCNT coating and the substrate was still smooth enough without etching to be able to utilize the thin film interference effect. Fig. 5 shows two samples deposited on as-received and etched Al substrates. The MWCNT coating on the etched substrate was not as uniform as the one on the as-received substrate. The better homogeneity on the as-received substrate could be explained by the thicker alumina coating on top of the substrate that would trap and result in better adhesion of the MWCNTs. Therefore, as-received optically smooth Al substrates were used for the rest of experiments.

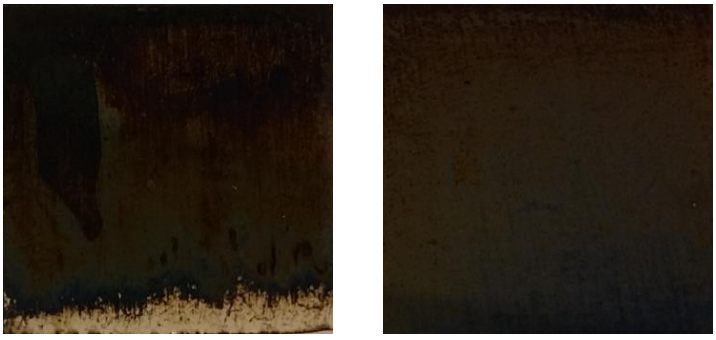

Fig. 5 MWCNT coatings deposited on etched (left) and as-received (right) Al substrates.

7.4 MWCNT absorbers without protective coating

Experiments were carried out to find the best recipe for heat treatment of the different types of MWCNT absorbers. The optimal peak temperature T_p and the dwell time t at T_p were determined to be 500 ℃ and 5 minutes for all three MWCNT absorbers. For N-CNT and P-CNT absorbers, the best spectral selectivity was achieved under the peak temperature and dwell time. Higher peak temperatures resulted in charring of MWCNTs, resulting in a loss of solar absorptance. T-CNT appeared to have a higher thermal stability than the former two MWCNTs. At a T_p of even 600 ℃ for T-CNT absorber, no obvious charring was observed, but the gained spectral selectivity was insignificant compared to that of the samples heat treated at 500 ℃. Details on this work can be found in *paper I* and *III*.

By adjusting the deposition time, various thicknesses of the three types of MWCNT absorbers were produced to study the effect of coating thickness on the solar absorptance and the thermal emittance. The effect on reflectance was quite similar for all three types of MWCNTs: with an increasing thickness, the reflectance in both the visible and infrared range was reduced, and the transition from low to high reflectance was shifted to longer wavelengths (Fig. 6). The resulting solar absorptance and thermal emittance are listed in Tab. 1. Fig. 7 shows how the spectral selectivity was influenced by MWCNT coating thickness. An optimal thickness for the best spectral selectivity existed for each MWCNT, which was about 1.7 μm for T-CNT, 0.48 μm for N-CNT and 0.23 μm for P-CNT. Consequently, the thinner N- and P-CNT absorber coatings can better utilize the advantages of thin film interference and get a sharper transition from low to high reflectance than the T-CNT absorber. It is worth noting that the results of the thickness measurement have a higher uncertainty for thinner coatings due to the inherent surface roughness of the aluminum substrates.

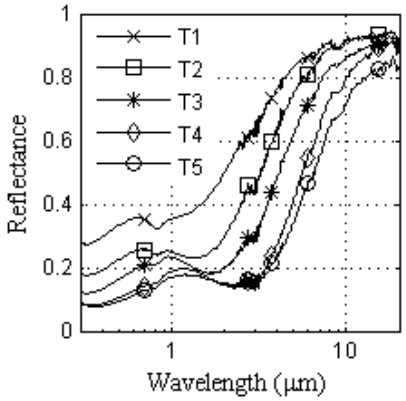

(a)

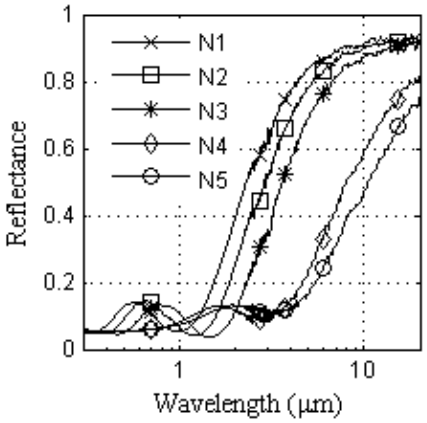

(b)

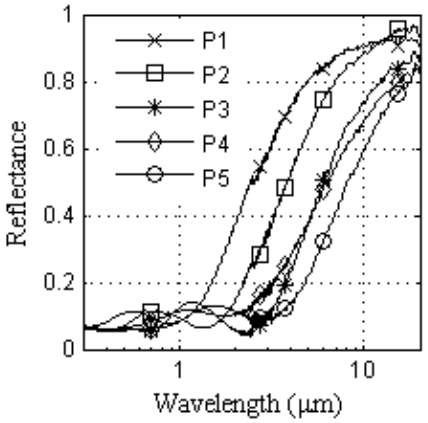

(c)

Fig. 6 The effect of coating thickness on the spectral reflectance of MWCNT absorbers: a) T-CNT absorbers; b) N-CNT absorbers; c) P-CNT absorbers.

Tab. 1: The effect of CNT coating thickness on solar absorptance and thermal emittance.

Samples		Coating thickness (μm)	α	ε
T-CNT absorbers	T1	0.95	0.71	0.11
	T2	1.41	0.79	0.19
	T3	1.61	0.85	0.29
	T4	1.70	0.87	0.30
	T5	1.93	0.91	0.50
N-CNT absorbers	N1	0.26	0.87	0.09
	N2	0.35	0.89	0.12
	N3	0.48	0.90	0.14
	N4	0.82	0.93	0.39
	N5	0.86	0.93	0.49
P-CNT absorbers	P1	0.19	0.87	0.11
	P2	0.23	0.90	0.13
	P3	0.49	0.92	0.27
	P4	0.50	0.91	0.31
	P5	0.55	0.92	0.39

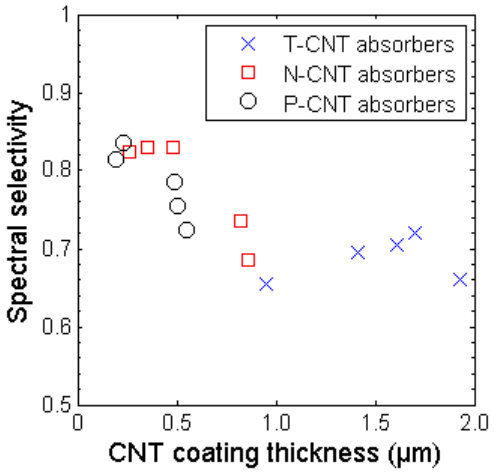

Fig. 7 Spectral selectivity of CNT absorbers vs CNT coating thickness.

7.5 Anti-reflection coated MWCNT absorbers

The results after AR coating have been reported in *paper IV*. The conclusion was that a porous silica layer coated on top of the MWCNT absorbers did enhance the solar absorption by depressing the peak reflectance in the visible range. A gain of 0.02 in solar absorptance was achieved. The only minor improvement achieved was suspected to be because of the mismatch of refractive indices between the PS layer and the MWCNT coating. Importantly, the porous layer also does not protect the underlying aluminum substrate from penetrating water which consequently will corrode.

7.6 MWCNT absorbers with protective coating

Four types of coatings were tested as the protective layer: silica, hybrid silica, 70/30 and 50/50 silica-titania. However, hybrid silica coated MWCNT absorber was not qualified in the condensation test and thus the results for this protective layer are not included in the following summary.

While a protective film shields the MWCNT coating and underlying Al substrate from the penetration of condensed water, the protective film also affects the optical properties of the MWCNT absorber. The three tested protective films of silica, 70/30 silica-titania and 50/50 silica-titania have different refractive indexes [120] and thus the effects on spectral reflectance of the absorber samples differ from each other.

Detailed results can be found in *paper V*. The conclusion was that the spectral selectivity of MWCNT absorbers coated with the optimal thickness of protective film had a slight gain for silica and 50/50 silica-titania films and kept unchanged for 70/30 silica-titania film. The only minor anti-reflective (AR) effect of the protective coatings is considered to be due to bad refractive index matching. The spectral reflectance of MWCNT absorbers before and after protective coating is displayed in Fig. 8.

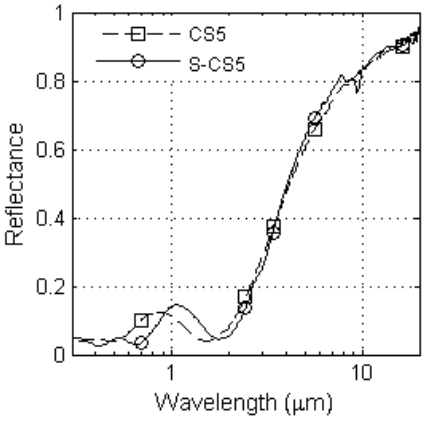

(a)

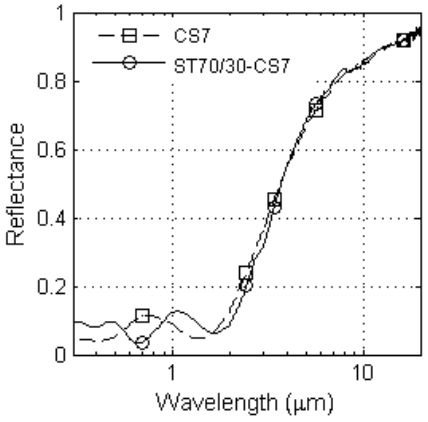

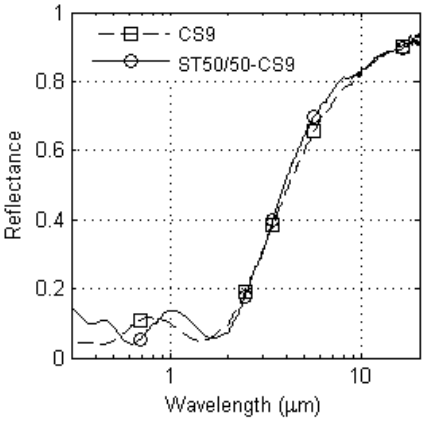

(b) (c)

Fig. 8 Reflectance spectra of MWCNT absorbers before (dashed curves) and after protective coating (solid curves): a) Silica; b) 70/30 Silica-titania; c) 50/50 Silica-titania.

(a)

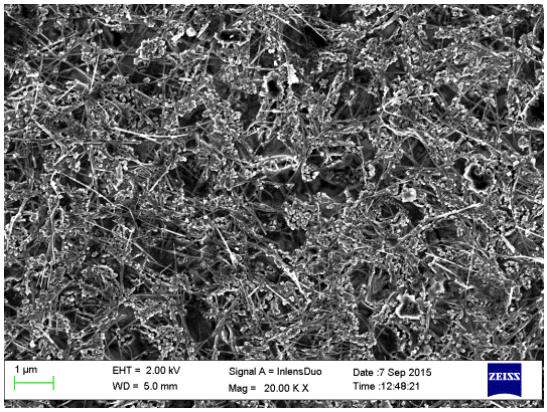

(b)

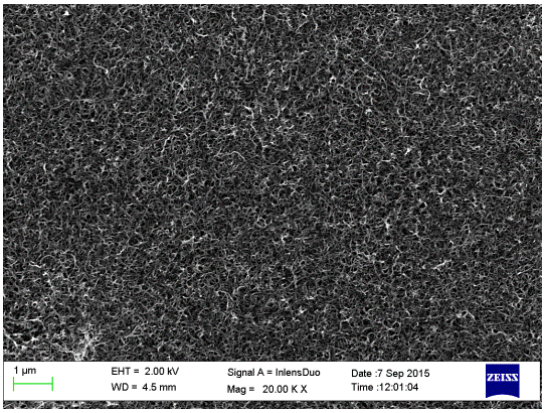

(c)

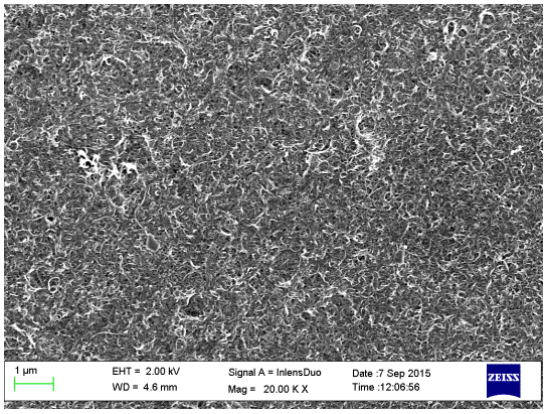

Fig. 9 SEM images of MWCNT absorbers under a magnification of 20 K, a) T-CNT absorber; b) N-CNT absorber; c) P-CNT absorber.

7.7 Surface morphology of MWCNT absorbers

Surface morphology of the three types of MWCNT absorbers and the respective shape of MWCNTs can be seen in Fig. 9. T-CNT coating (Fig. 9a) had a very different surface appearance from those modes of N-CNT and P-CNT (Fig. 9b and 9c). The deposited T-CNTs were stretched and mostly parallel to the Al substrate. The MWCNT coating was embedded with carbon impurities and the surfactant. N-CNTs and P-CNTs were curved and nested like cotton, resulting in better light trapping i.e. higher absorption of solar radiation. Compared to N-CNT and P-CNT absorbers, T-CNT absorbers had a lower density of MWCNT and a lower coverage of the substrate, which resulted in a rougher surface. The lower density of T-CNTs was the main reason for the increased optimal thickness compared to N- and P-CNT. The lower CNT coverage of the substrate from T-CNTs is also evidenced by the visible interband absorption dip of aluminum at about 830 nm [121] as indicated in Fig. 6a and sample T1-T3 (Section7.4). The lower density of CNT might be due to a lower purification from original as-produced CNTs or a higher surfactant concentration in the CNT suspension.

7.8 Energy dispersive X-ray spectroscopy

Fig. 10 displays the EDS results of three types of MWCNT absorbers. The detected aluminum content originated from the substrate. The MWCNT coatings contained mainly carbon. The oxygen content originated from the oxidation of Al substrate, functional groups of MWCNTs and the residual surfactant. Only the surfactant contained sulfur. T-CNT coatings had a higher concentration of sulfur and oxygen due to a greater amount of surfactant left in the coating, compared to N-CNT and P-CNT coatings. This confirmed the suspicion of higher surfactant concentrations for T-CNT suspensions based on the SEM image. EDS analysis results indicated a sulfur content of about 1.7 wt. % in T-CNT coatings after heat treatment. The value is much higher than that in N-CNT and P-CNT coatings, which is no more than about 0.6 wt. %.

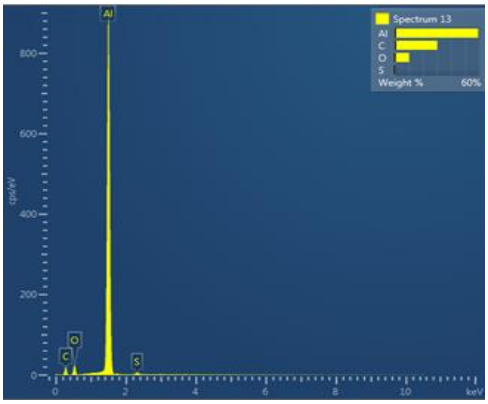

(a)

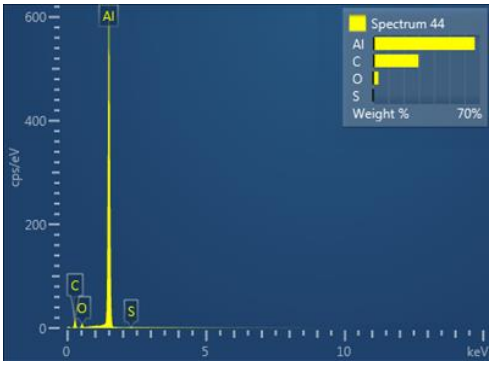

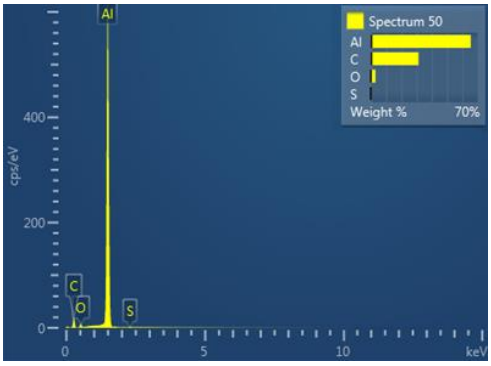

(b) (c)

Fig. 10 EDS results of MWCNT absorbers after heat treatment. a) T-CNT absorber; b) N-CNT absorber; c) P-CNT absorber.

8. Accelerated ageing results

The results from the condensation test and thermal stability tests are summarized here. The long-term durability of different MWCNT solar absorbers was assessed according to the procedure described in Section 4.4. While the MWCNT absorbers performed well in the thermal stability test, their resistance to condensed water was poor, due to oxidation of the underlying Al substrate. Coated with dense protective coatings, the durability was significantly improved. All details can be found in *paper V*.

8.1 Condensation test

8.1.1 MWCNT absorbers

The test revealed that all three types of solar absorbers -- T-CNT, N-CNT and P-CNT absorbers had poor resistance to condensation. Fig. 11 presents the spectral reflectance of the MWCNT absorber samples before and after subjection to a condensation test of 150 h duration. It can be seen that condensed water on the sample surface had a serious impact on the spectral reflectance, especially in the IR wavelength region. The solar absorptance had not changed and remained at 0.87, 0.91 and 0.91for the T-CNT, N-CNT and P-CNT absorber respectively. The peak reflectance occurring in the high intensity region of the solar spectrum was reduced and the reflectance in the near infrared range increased. The spectral reflectance in the far infrared range decreased significantly. As a consequence, the thermal emittance increased from 0.31 to 0.89 for the T-CNT absorber, from 0.16 to 0.86 for the N-CNT absorber and from 0.17 to 0.85 for the P-CNT absorber after the condensation test. The resulting PC values were much higher than the limit of 0.015 for qualification (shown in Tab. 2). The increased absorption in the infrared range is in all probability caused by the oxidation of the underlying aluminum substrate [122]. This is confirmed by an EDS analysis. The oxygen content of MWCNT absorber after condensation test was much higher than that of MWCNT absorber before condensation test (See paper V for detailed results). Due to the porosity of MWCNT coating, the condensed water was able to pass through the coating to form an aluminum hydroxide or oxo-hydroxide through oxidation. The rate of oxidation was accelerated by the elevated test temperature of 40 ℃. It is

considered unlikely that the condensation test oxidizes the MWCNTs themselves. Usually strongly acidic conditions need to be present in order for that to take place [123]. The surface of the samples appeared to be slightly rougher after the condensation test. This resulted in more light scattering which could explain the increase in absorption in the visible wavelength range, as shown in Fig. 11.

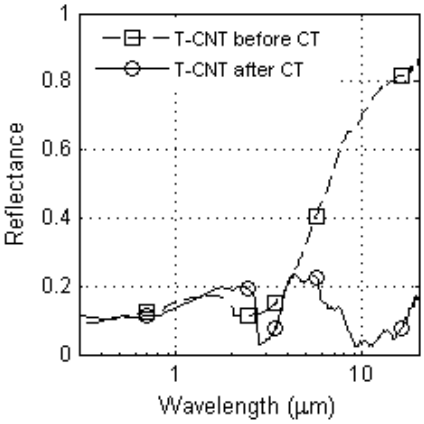

(a)

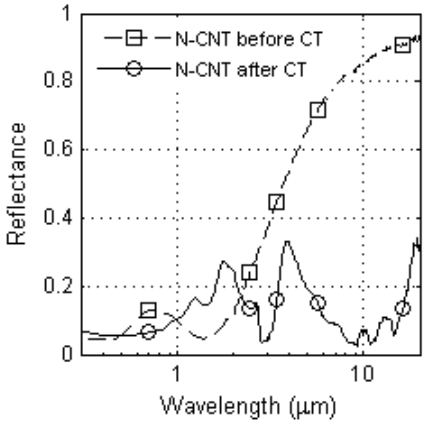

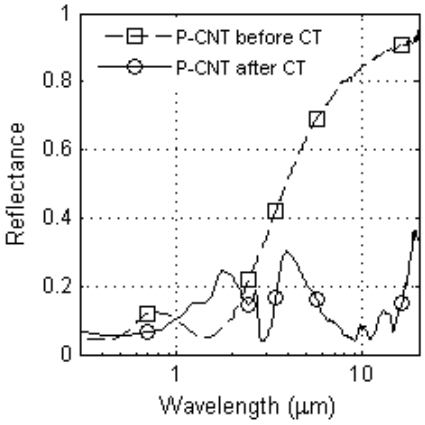

(b) (c)

Fig. 11 The spectral reflectance of MWCNT absorbers before (dashed curves) and after (solid curves) 150 hours of condensation test. (a) T-CNT absorber; (b) N-CNT absorber; (c) P-CNT absorber.

Tab. 2 PC values after 150 hours of condensation test.

Sample type	Before condensation test		After condensation test		PC
	α	ε	α	ε	
T-CNT absorber	0.87	0.31	0.87	0.89	0.29
N-CNT absorber	0.91	0.16	0.91	0.86	0.35
P-CNT absorber	0.91	0.17	0.91	0.85	0.34

8.1.2 MWCNT absorbers with protective coating

It was judged sufficient to only use one type of absorbers (N-CNT) to prove the effectiveness of the protective coatings. Three different types of protective films were tested: silica, 70/30 and 50/50 silica. The results from the three protective films were reported in *paper V*. A brief conclusion was that the durability of the N-CNT absorber was significantly improved after coated with silica, 70/30 and 50/50 silica-titania films. The resulting PC values after 600 hours of condensation testing were only 0.002, 0.013 and 0.014, respectively for silica, 70/30 and 50/50 silica-titania film coated absorbers. Therefore, they are considered as qualified as long as the adhesion requirements are met which was not tested in the scope of the current work.

8.2 Thermal stability test

8.2.1 MWCNT absorbers

The thermal stability test was carried out only on N-CNT and P-CNT absorbers since their spectral selectivity was much higher than that of T-CNT absorber.

Both MWCNT absorbers performed well in thermal stability test. After 150 hours' testing, the spectral reflectance was barely changed in the entire measured wavelength range (Fig. 12). This was expected since the MWCNT coatings were heat treated at 500 ℃ in air prior to the thermal stability test and consequently should be thermally stable at the much lower test temperature of 265 ℃.

Due to the very low PC values after 150 hours of thermal stability testing, further testing was not performed.

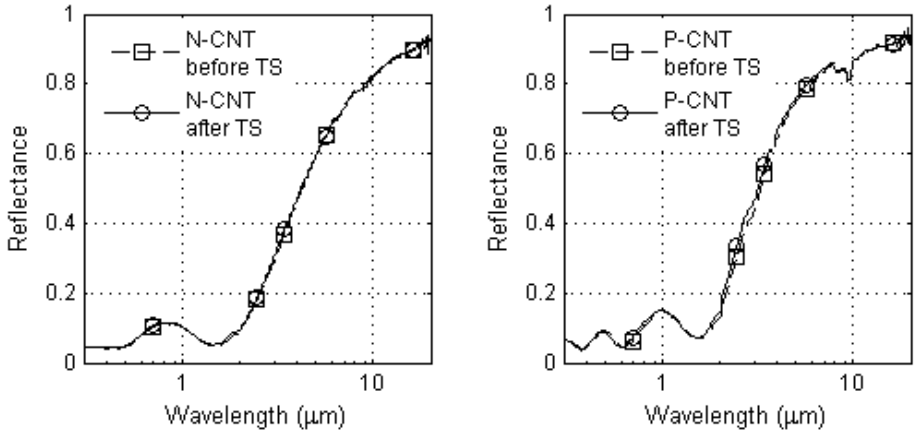

(a) (b)

Fig. 12 The spectral reflectance of MWCNT absorbers before (dashed curves) and after (solid curves) 150 hours of thermal stability test. (a) N-CNT absorber; (b) P-CNT absorber.

8.2.2 MWCNT absorbers with protective coating

Protective film coated N-CNT absorbers also showed good stability at high temperature. The results were reported in Paper V. Similar to the samples without protective films, the spectral reflectance remained almost unaffected in the UV-Vis-NIR spectrum for all the protective film coated samples after 600 hours of thermal stability test. There was a slightly reduced thermal emittance due to higher reflectance in the infrared range i.e. little improvement on spectral selectivity. The PC values attained after 600 hours were -0.002, -0.007 and 0.002 for MWCNT absorbers coated with silica, 70/30 silica-titania and 50/50 silica-titania respectively. The negative values indicate a small improvement of performance after 600 hours of thermal stability testing.

9. Concluding remarks

A novel spectrally selective solar absorber using multi-walled carbon nanotube (MWCNT) as absorbing layer was fabricated. The MWCNT coatings were prepared by electrophoretic deposition (EPD) on specularly reflective aluminum substrates. SEM imaging showed that the coatings were homogenous on the surface. The fabricated MWCNT solar absorbers exhibited good spectral selectivity over the solar and infrared spectrum, which indicates that MWCNT is a potential candidate for use as a spectrally selective absorber in solar thermal collectors. Three different types of MWCNT were investigated: T-CNT, N-CNT and P-CNT. The thickness of MWCNT coatings increased linearly with the deposition time. With thicker MWCNT coatings, the transition from low to high reflectance of solar absorbers shifted to longer wavelengths which benefited the solar absorptance but simultaneously increased the thermal emittance. The thickness at the optimal spectral selectivity was lower for the solar absorbers using N-CNT and P-CNT, and was in a range of few hundreds of nanometers. SEM investigation revealed that, after heat treatment nearly pure N-CNTs and P-CNTs were left in the MWCNT coatings while T-CNTs were embedded in a large amount of impurities. The optimal solar absorptance and thermal emittance achieved by the solar absorber with a single MWCNT coating were 0.88 and 0.28 for T-CNT, 0.90 and 0.14 for N-CNT, 0.90 and 0.13 for P-CNT. These results are slightly under par with the performance of popular commercial absorber products but still competitive because of the production methods advantages.

A voltage threshold for EPD was found to be 15 V for the MWCNT suspension systems used. The MWCNT coatings exhibited poor homogeneity when deposited below the voltage threshold. EPD proved to be a fast cheap and facile method of preparing CNT coatings. Compared to the traditional processes of fabricating spectrally selective absorbers, EPD is very fast and is more environmentally-friendly due to the type of aqueous suspensions and low chemical consumption used. However, care have to be taken when handling dry unbound CNT, before they are made into a suspension, since they adversely can affect our health and respiratory system. In addition, the production process does not require any advanced coating production equipment and the absorbers only need to be heat treated in air, without a need for an inert atmosphere.

Porous silica layers were tested as anti-reflection coatings for the MWCNT absorbers. A maximum gain of 0.02 on solar absorptance was achieved. The only minor improvement was suspected to be because of the mismatch of refractive indices between the PS layer and the MWCNT coating.

Accelerated ageing tests have revealed that MWCNT absorbers with bare MWCNT coatings have excellent thermal stability. However, the absorbers cannot withstand the penetration of condensed water which causes oxidation of the underlying aluminum substrate. The oxidation results in significantly increased thermal emittance, i.e. degraded spectral selectivity. The MWCNT absorbers were therefore disqualified. In order to prevent penetration of water through the CNT layer, protective silica and silica-titania thin films were coated on the top of MWCNT absorbers. The experiments have shown very promising results. Having these protective films, the solar absorptance and the thermal emittance of the MWCNT absorbers were almost not impacted at all by the condensation tests. All three protective film coated MWCNT absorbers were qualified in accelerated ageing tests.

In conclusion, this work has provided a new approach to manufacturing high performance spectrally selective solar thermal absorbers. The production method is simple, very fast, inexpensive and environmentally friendly and competitive to existing alternatives.

10. Future outlook

This chapter discusses issues related to the continuation of this work, including potential commercialization and the possible improvements.

Since the MWCNT absorbers have a good performance which is in line or slightly under par with currently popular products and exhibit an excellent long-term durability, there is a potential for industrial production. Owing to the simple and very fast production method and low MWCNT consumption, MWCNT absorbers could be cost competitive compared with existing absorbers. A market survey and comprehensive cost calculation are required for further assessment of industrial production. In addition, large scale manufacturing issues have not been addressed in this work. How large scale industrially efficient EPD production of CNT coatings on Al substrates can be performed must be studied.

MWCNT coatings containing nearly pure MWCNTs were prepared. Measurement of their optical constants has been attempted without satisfactory results. It is assumed that there are many factors affecting the optical properties of MWCNT coatings, for example the chirality, diameter and length of MWCNTs, deposited position on the substrate and coating thickness. However, knowing the optical constants of a specific MWCNT coating is still of great value for the computational design and optimization, as well as for the selection of anti-reflection coating. Ellipsometry is a proven method of measuring optical constants and has been utilized in this work. However, the method was challenging on this type of thin films and the results had a high uncertainty. Other methods for properly modelling the MWCNT coating are expected to improve the reliability of the results.

Nanoporous silica film has been reported to have a low refractive index of 1.2 – 1.3 ascribed to the introduced porosity [124]. However, the experiment results from porous silica coating tested in this work are not convincing. Further work is needed to achieve better refractive index matching and improvement. It is worth noting that an addition of a nanoporous anti-reflection coating has to involve a further surface treatment in order to qualify the coated absorber in accelerated ageing tests since condensed water normally is able to penetrate porous films.

SEM images have illustrated two different surface morphologies of MWCNT absorbers produced in this work which resulted in the differences in solar absorptance and thermal emittance. Due to the limited time, the correlation between MWCNT morphology and absorber performance has not been completely studied. More experiments can be carried out for better understanding.

This work has only focused on the application of CNTs as an absorbing layer for spectrally selective solar thermal absorbers. Potential applications can be explored in other areas of thermal energy management, PV or as sensors.

11. Acknowledgements

First of all, I would like to sincerely thank my supervisor Prof. Tobias Boström for his high-performance guidance and all the support that led to the completion of this thesis. I am grateful to him and Mr. Terje Nordvåg, administration director at Norut Narvik, for giving me the opportunity to pursue my Ph. D degree. I am grateful to the project leader Dr. Quang Hong Nguyen for his support and the discussion on experiments. The company ASV Solar AS provided part of the funding for this project and I wish to take this opportunity to express my gratitude to them.

I place my sincere gratitude to my colleagues at Norut Narvik: Dr. Christian Petrich, Tore Pettersen, Dr. Ross Wakelin, Dagfinn Johnsen and Kjell Ellingsen for their help and support. I would also express my thanks to Dr. Nga Dang Phong, Bård Arntsen, Øystein Kleven, Hanna Persson and other colleagues at Norut Narvik for their encouragement and chatting.

I acknowledge Dilip Chithambaranadhan's support in programming Matlab codes for generating reflectance curves and the calculation of solar absorptance and thermal emittance values.

Many thanks need be addressed to Tom-Ivar Eilertsen and Øystein Jordheim at The Arctic University of Norway for their assistance with measurements and analyses which were valuable for my PhD study.

But most of all I would like to thank my parents, my wife and my two lovely boys for the encouragement and the endless love! Especially my wife, she has always been there for me. Without her being together with me, all this would have been impossible.

The work presented in this thesis is financed by the Nano2021 program of the Research Council of Norway (Project number 219161) and ASV Solar AS. The study has been carried out at Northern Research Institute Narvik AS (Norut Narvik) and at the department of Physics and Technology, The Arctic University of Norway, Tromsø, Norway.

12. References

[1] REN21. 2015. Renewables 2015 Global Status Report (Paris: REN21 Secretariat). ISBN 978-3-9815934-6-4.

[2] B. Orel, Z. Crnjak Orel, R. Jerman. Coil-coating paints for solar collector panels – II. FT-IR spectroscopic investigations. Solar & Wind Technology Vol. 7, No. 6, pp. 713-717, 1990.

[3] J. El Nady et al., Nanoparticles Ni electroplating and black paint for solar collector applications, Alexandria Eng. J. (2016), http://dx.doi.org/ 10.1016/j.aej.20 15.12.029.

[4] K. Shanker, P. H. Holloway. Electrodeposition of black chrome selective solar absorber coatings with improved thermal stability. Thin Solid Films, 127 (1985) 181-189.

[5] R.L. Axelbaum, H. Brandt. The effect of substrate surface preparation on the optical properties of a black chrome solar absorber coating. Solar Energy Vol. 39 No. 3, pp. 233-241, 1987.

[6] K. N. Srinivasan, N.V. Shanmugam, M. Selvam, S. John, B. A. Shenoi. Nickel-black solar absorber coatings. Energy Convers. Mgmt vol. 24, No. 4 pp. 255-258, 1984.

[7] M. Lira-Cantu´, A. M. Sabio, A. Brustenga, P. Go´mez-Romero. Electrochemical deposition of black nickel solar absorber coatings on stainless steel AISI316L for thermal solar cells. Solar Energy Materials and Solar Cells 87 (2005) 685–694.

[8] L. Zheng, F. Zhou, Z. Zhou, X. Song, G. Dong, M. Wang, X. Diao. Angular solar absorptance and thermal stability of Mo–SiO2 double cermet solar selective absorber coating. Solar Energy 115 (2015) 341–346.

[9] L. Rebouta, A. Sousa, P. Capela, M. Andritschky, P. Santilli, A. Matilainen, K. Pischow, N.P. Barradas, E. Alves. Solar selective absorbers based on Al2O3:W cermets and AlSiN/AlSiON layers. Solar Energy Materials and Solar Cells 137 (2015) 93–100.

[10] T. Boström, G. Westin and E. Wäckelgård. Optimization of a solution-chemically derived solar absorbing spectrally selective surface. Solar Energy Materials and Solar Cells, 91 (2007) 38-43.

[11] M.G. Hutchins. Spectrally selective solar absorber coatings. Applied Energy (1979) 0306-2619/79/0005-0251.

[12] P. Yianoulis, M. Giannouli, Kalogirou SA. 2012. Solar selective coatings. Comprehensive Renewable Energy, Volume 3. Doi: 10.1016/B978-0-08-087872-0.00309-7.

[13] Gordon J. 2001. Solar Energy, The State of the Art, James & James Ltd., London.

[14] T. Boström, G. Westin, E. Wäckelgård. Solution-chemical derived nickel-alumina coatings for thermal solar absorbers. Solar Energy 74 (2003) 497-503.

[15] L. Besra, M. Liu. A review on fundamentals and applications of electrophoretic deposition (EPD). Progress in Materials Science 52 (2007) 1–61.

[16] B. Ferrari, R. Moreno, EPD kinetics: A review. Journal of the European Ceramic Society 30 (2010) 1069–1078.

[17] S. S. Tinchev, P. I. Nikolova, Y. T. Dyulgerska, Thermal solar absorber made of diamond-like carbon thin films. Journal of Physics: Conference Series 223 (2010) 012017.

[18] P. Konttinen, T. Salo, P.D. Lund, Degradation of unglazed rough graphite-aluminium solar absorber surfaces in simulated acid and neutral rain. Solar Energy78 (2005) 41–48.

[19] R. Kunič, M. Koželj, B. Orel, A. Šurca Vuk, A. Vilčnik, L. Slemenik Perše, D. Merlini, S. Brunold. Adhesion and thermal stability of thickness insensitive spectrally selective (TISS) polyurethane-based paint coatings on copper substrates. Solar Energy Materials & Solar Cells 93 (2009) 630–640.

[20] Planck, M. 1914. The Theory of Heat Radiation. Masius, M. (transl.) (2nd ed.). P. Blakiston's Son & Co.

[21] NASA Solar System Exploration –Sun: Facts & Figures. Retrieved 19 January 2016. http://solarsystem.nasa.gov/planets/sun/facts.

[22] J. Nelson. The Physics of Solar Cells. 2003. Imperial Colleage Press: London.

[23] ISO 9845-1: 1992 (en) Solar energy – Reference solar spectral irradiance at the ground at different receiving conditions – Part 1: Direct normal and hemispherical solar irradiance for air mass 1.5.

[24] T. Boström. Solution-Chemically Derived Spectrally Selective Solar absorbers. 2006. Uppsala University: Uppsala. ISBN: 91-554-6663-X.

[25] ISO22975-3:2014.Solar energy – collector components and materials – Part 3: absorber surface durability.

[26] B.Carlsson. Recommended qualification test procedure for solar absorber surface durability, IEA SHC Task27 Draft Report, 2004.

[27] Kennedy C.E. (2002) Review of mid-to high-temperature solar selective absorber materials. Technical Report NREL/TP-520-31267. Golden, CO: National Renewable Energy Laboratory.

[28] B. S. Richard and D. C. George, Optical reflectance and transmission of a textured surface, Thin Solid Films, 45 (1977) 19-29.

[29] G. L. Harding and M.R. Lake, Sputter etched metal solar selective absorbing surfaces for high temperature thermal collectors, Solar Energy Materials, 5 (1981) 445-464.

[30] G. L. Harding. Evaporated chromium black selective solar absorbers. Thin Solid Film, 38 (1976) 109-115

[31] S. Eugénio, C. M. Rangel, R. Vilar, A. M. Botelho do Rego. Electrodeposition of black chromium spectrally selective coatings from a Cr(III)–ionic liquid solution. Thin Solid Films 519 (2011) 1845–1850.

[32] S. Survilienė, A. Češūnienė, R. Juškėnas, A. Selskienė, D. Bučinskienė, P. Kalinauskas, K. Juškevičius, I. Jurevičiūtė. Applied Surface Science 305 (2014) 492–497.

[33] T. Karlsson, A. Roos. Optical properties and spectral selectivity of copper oxide on stainless steel. Solar Energy Materials 10 (1984) 105-119.

[34] X. Xiao, L. Miao, G. Xu, L. Lu, Z. Su, N. Wang, S. Tanemura. A facile process to prepare copper oxide thin films as solar selective absorbers. Applied Surface Science 257 (2011) 10729– 10736.

[35] S. Karthick Kumar, S. Suresh, S. Murugesan, S.Paul Raj. CuO thin films made of nanofibers for solar selective absorber applications. Solar Energy 94 (2013) 299–304.

[36] T. Maruyama, T. Nakai. Cobalt oxide thin films prepared by chemical vapor deposition from cobalt (II) acetate. Solar Energy Materials 23 (1991) 25-29.

[37] E. C. Barrera, T. G. Viveros, U. Morales. Preparation of selective surfaces of black cobalt by the sol-gel process. WREC 1996.

[38] C. Choudhury, H. K. Sehgal. Black cobalt selective coatings by spray pyrolysis for photothermal conversion of solar energy. Solar Energy 28 (1982) 25-31.

[39] E. Ienei, L. Isac, C. Cazan, A. Duta. Characterization of Al/Al2O3/NiOx solar absorber obtained by spray pyrolysis. Solid State Sciences 12 (2010) 1894-1897.

[40] L. Kaluža, A. Šurca-vuk, B. Orel. Structural and IR spectroscopic analysis of sol-gel processed CuFeMnO4 spinel and CuFeMnO4/silica films for solar absorbers. Journal of Sol-Gel Science and Technology 20 (2001) 61-83.

[41] A. Cao, X. Zhang, C. Xu, B. Wei, C. Wu. Tandem structure of aligned carbon nanotubes on Au and its solar thermal absorption. Solar Energy Materials & Solar Cells 70 (2002) 481–486

[42] N. Selvakumar , S. B. Krupanidhi , and Harish C. Barshilia. Carbon Nanotube-Based Tandem Absorber with Tunable Spectral Selectivity: Transition from Near-Perfect Blackbody Absorber to Solar Selective Absorber. Adv. Mater. 2014, 26, 2552–2557.

[43] O.S. Heavens. Optical properties of thin solid films. 1991. Dover Publications. New York. ISBN: 9780-48666924

[44] H. H. Li. Refractive index of alkaline earth halides and its wavelength and temperature derivatives. J. Phys. Chem. Ref. 9 (1980) 161-289 .

[45] L. Gao, F. Lemarchand, M. Lequime. Refractive index determination of SiO2 layer in the UV/Vis/NIR range: spectrophotometric reverse engineering on single and bi-layer designs, J. Europ. Opt. Soc. Rap. Public. 8 (2013) 13010.

[46] S. Guldin. Inorganic nanoarchitectures by organic self-assembly. 2013. Springer Theses, DOI: 10.1007/978-3-319-00312-2_2.

[47] A. Mahdjoub, L. Zighed. New designs for graded refractive index antireflection coatings. Thin Solid Films 478 (2005) 299-304.

[48] C. F. Bohren, D. R. Huffman. Absorption and Scattering of Light by Small Particles. (2004) Wiley-VCH. Weinheim. ISBN-13: 978-0-471-29340-8.

[49] C. M. Lampert. Coatings for enhanced photothermal energy collection. Solar Energy Materials 1 (1979) 319-341.

[50] T. Stöckli, Z. L. Wang, J. M. Bonard, P. Stadelmann, A. Châtelain. Plasmon excitations in carbon nanotubes. Philosophical Magzine B 79 (1999) 1531-1548.

[51] Katumba G, Lu J, Olumekor L, Westin G, Wäckelgård E. Low cost selective solar absorber coatings: characteristics of carbon-in-silica synthesized with sol-gel technique. Journal of Sol-Gel Science and Technology 36 (2005) 33-43.

[52] P. Konttinen, T. Shao, P. D. Lund. Degradation of unglazed rough graphite-aluminium solar absorber surfaces in simulated acid and neutral rain. Solar Energy 78 (2005) 41-48.

[53] http://www.fluxim.com/

[54] A. D. Rakić. Algorithm for the determination of intrinsic optical constants of metal films: application to aluminum. Applied Optics 34 (1995) 4755-4767.

[55] A. Borghesi, G. Guizzetti, Graphite (C). Handbook of Optical Constants and Solids II (1991) 449-460.

[56] F. Rouleau, P. G. Martin. Shape and clustering effects of the optical properties of amorphous carbon. The Astrophysical Journal 377 (1991) 526-540.

[57] H. Soetedjo, M. F. Mora, C. D. Garcia. Optical properties of single-wall carbon nanotube films deposited on Si/SiO2 wafers. Thin Solid Films 518 (2010) 3954–3959.

[58] K. Gharbavi, H. Badehian. Optical spectra of zigzag carbon nanotubes. Optik 127 (2016) 6952–6960.

[59] M. M. Rahman, H. Younes, G. Ni, T. Zhang, A. A. Ghaferi. Sythesis and optical characterization of carbon nanotube arrays. Materials Research Bulletin 77 (2016) 243–252.

[60] Y. Murakami, E. Einarsson, T. Edamura, S. Maruyama. Polarization dependent optical absorption properties of single-walled carbon nanotubes and methodology for the evaluation of their morphology. Carbon 43 (2005) 2664–2676.

[61] H. G. Tompkins, E. A. Irene. Handbook of Ellipsometry. William Andrew. New York. ISBN: 0-8155-1499-9.

[62] Z. Chen, T. Boström. Electrophoretically deposited carbon nanotube spectrally selective solar absorbers. Solar Energy Materials & Solar Cells 144 (2016) 678–683.

[63] Z. Chen, T. Boström. Accelerated Ageing Tests of Carbon Nanotube Spectrally Selective Solar absorbers. Solar Energy Materials & Solar Cells. Submitted.

[64] J. Bartl, M. Baranek. Emissivity of aluminium and its importance for radiometric measurement. Measurement Science Review 4 (2004) 31-36.

[65] S. Iijima. Helical microtubules of graphitic carbon. Nature 354 (1991) 56–58.

[66] L. Chen, H. Xie, W. Y. (2011). Functionalization Methods of Carbon Nanotubes and Its Applications, Carbon Nanotubes Applications on Electron Devices, Prof. Jose Mauricio Marulanda (Ed.), ISBN:978-953-307-496-2, InTech, Available from: http://www.intechopen.com/books/carbon-nanotubes-applicationson-electron-devices/functionalization-methods-of-carbon-nanotubes-and-its-applications.

[67] A. Zettl. Chapter 1. Nanotubes: An Experimental overview. Carbon Nanotubes: Quantum Cylinders of Graphene. 2008. ISSN: 1572-0934/doi:10.1016/S1572-0934(08)00001-2.

[68] D. Qian, G. J. Wagner, W. H. Liu. Mechanics of carbon nanotubes. Appl. Mech. Rev. 55 (2002) 495-533.

[69] M. M. J. Treacy, T.W. Ebbesen, J.M. Gibson. Exceptionally high Young's modulus observed for individual carbon nanotubes. Nature 381 (1996) 678-680

[70] M. Terrones. Carbon nanotubes, synthesis and properties, electronic devices and other emerging applications. International Materials Reviews 49 (2004) 325-332.

[71] S. Berber, Y. Kwon, D. Tománek. Unusually high thermal conductivity of carbon nanotubes. Physical Review Letters 84 (2000) 4613-4616.

[72] J. Hone. Carbon nanotubes: thermal properties. (2007) Marcel Dekker Inc. New York.

[73] B. Rezaei, O. Rahmannian, A. A. Ensafi. An electrochemical sensor based on multiwall carbon nanotubes andmolecular imprinting strategy for warfarin recognition anddetermination. Sensors and Actuators B 196 (2014) 539–545.

[74] Y. Li. T, Wu, M. Yang. Humidity sensors based on the composite of multi-walled carbonnanotubes and crosslinked polyelectrolyte with good sensitivity andcapability of detecting low humidity. Sensors and Actuators B 203 (2014) 63–70.

[75] S. J. Oh, J. Zhang, Y. Cheng, H. Shimoda, O. Zhou. Liquid-phase fabrication of patterned carbon nanotube field emission cathodes. Appl. Phys. Lett. 84, 3738 (2004); doi: 10.1063/1.1737074.

[76] C. Niu, E. K. Sichel, R. Hoch, D. Moy, H. Tennent. High power electrochemical capacitors based on carbon nanotube electrodes. Appl. Phys. Lett. 70, 1480 (1997); doi: 10.1063/1.118568.

[77] A. T. Lawal. Synthesis and utilization of carbon nanotubes for fabrication of electrochemical biosensors. Materials Research Bulletin 73 (2016) 308–350.

[78] M. I. Sajid, U. Jamshaid, T. Jamshaid, N. Zafar, H. Fessi, A. Elaissari. Carbon nanotubes from synthesis to in vivo biomedical applications. International Journal of Pharmaceutics 501 (2016) 278–299.

[79] G. Yamamoto, M. Omori, T. Hashida, H. Kimura. A novel structure for carbon nanotube reinforced alumina composites with improved mechanical properties. Nanotechnology 19 (2008) 315708 (7pp).

[80] L. Berguiga, J. Bellessa, F. Vocanson, E. Bernstein, J.C. Plenet. Carbon nanotube silica glass composites in thin films by the sol–gel technique. Optical Materials 28 (2006) 167–171.

[81] G. Krishnamurthy, R. Namitha, A. Sarika. Synthesis of carbon nanotubes and carbon spheres and study of their hydrogen storage property by electrochemical method. Procedia Materials Science 5 (2014) 1056 – 1065.

[82] S. H. Barghi, T. T. Tsotsis, M. Sahimi. Chemisorption, physisorption and hysteresis during hydrogen storage in carbon nanotubes. International Journal of Hydrogen Energy 39 (2014) 1390-1397.

[83] M. A. Peacock, C. K. Roy, M. C. Hamilton, R. W. Johnson c, R. W. Knight, D. K. Harris. Characterization of transferred vertically aligned carbon nanotubes arrays as thermal interface materials. International Journal of Heat and Mass Transfer 97 (2016) 94-100.

[84] K. Pielichowska, K. Pielichowski. Phase change materials for thermal energy storage. Progress in Materials Science 65 (2014) 67-123.

[85] P. Mierczynski, K. Vasilev, A. Mierczynska, W. Maniukiewica, M. I. Szynkowska, T. P. Maniecki. Bimetallic Au–Cu, Au–Ni catalysts supported on MWCNTs foroxy-steam reforming of methanol. Applied Catalysis B: Environmental 185 (2016) 281–294.

[86] W. Chen, Z.Fan, X. Pan, X. Bao. Effect of confinement in carbon nanotubes on the activity of Fisher-Tropsch iron catalyst. J. AM. CHEM. SOC 130 (2008) 9414–9419.

[87] M. F. L. De Volder, S. H. Tawfick, R. H. Baughman, A. J. Hart. Carbon nanotubes: present and future commercial applications. Science 339 (2013) 535-539.

[88] J. Kolosnjaj, H. Szwarc, F. Moussa. Toxicity studies of carbon nanotubes. Bio-Applications of Nanoparticles, W. C. W. Chan, 2007. Landes Bioscience, Texas. ISBN 978-0-387-76712-3.

[89] C. Lam, J. T. James, R. McCluskey, S. Arepalli, R. L. Hunter. A review of carbon nanotubes toxicity and assessment of potential occupational and environmental health risks. Critical Reviews in Toxicology 36 (2006) 189-217.

[90] C. O. Robichaud, D. Tanzil, U. Weilenmann, M. R. Wiesner. Relative risk analysis of several manufactured nanomaterials: an insurance industry context. Environ. Sci. Technol 39 (2005) 8985-8994

[91] J. Hilding, E. A. Grulke, Z. G. Zhang, F. Lockwood. Dispersion of carbon nanotubes in liquids. Journal of Dis. Sci. and Tec. 24 (2003) 1-41.

[92] D. Lin, N. Liu, K. Yang, B. Xing, F. Wu. Different stabilities of multiwalled carbon nanotubes in fresh surface water samples. Environmental Pollution 158 (2010) 1270-1274.

[93] H. Wang. Dispersing carbon nanotubes using surfactants. Current Opinion in Colloid & Interface Science 14 (2009) 364–37.

[94] Y. Y. Huang, E. M. Terentjev. Dispersion of carbon nanotubes: mixing, sonication, stabilization and composite properties. Polymers 2012, 4, 275-295; doi:10.3390/polym4010275.

[95] P. C. Hiemenz, R. Rajagopalan. Principles of colloid and surface chemistry (Third edition). 1997. CRC Press. Boca Raton, ISBN-10: 0-8247-9397-8.

[96] L. Vaisman, H. D. Wagner, G. Marom. The role of surfactants in dispersion of carbon nanotubes. Advances in Colloid and Interface Science 128–130 (2006) 37–46.

[97] E. E. Tkalya, M. Ghislandi, G. De With, C. E. Koning. The use of surfactants for dispersing carbon nanotubes and graphene to make conductive nanocomposites. Current Opinion in Colloid & Interface Science 17 (2012) 225–232.

[98] A. Schierz, H. Zänker. Aqueous suspensions of carbon nanotubes: surface oxidation, colloidal stability and uranium sorption. Environmental Pollution 157 (2009) 1088–1094.

[99] K. Holmberg, B. Jönsson, B. Kronberg, B. Lindman. Surfactants and polymers in aqueous solution (Second Edition). 2002. John Wiley & Sons, Ltd. Chichester. ISBN: 0-471-49883-1.

[100] M. M. Singer, R. S. Tjeerdema. Fate and effects of the surfactant sodium dodecyl surfate. Reviews of Environmental Contamination and Toxicology 133 (1993) 95-149.

[101] J.H. Kay, F. E. Kohn, J. C. Calandra. Subacute oral toxicity of a biodegradable, linear alkylbenzene sulfonate. Toxicology and Applied Pharmacology 7, 812-818 (1965).

[102] D. R. Karsa, M. R. Porter. Biodegradability of surfactants. Springer. 1995. ISBN: 978-94-011-1348-9.

[103] L. Jiang, L. Gao, J. Sun. Production of aqueous colloidal dispersions of carbon nanotubes. Journal of Colloid and Interface Science 260 (2003) 89–94.

[104] L. Ju, W. Zhang, X. Wang, J. Hu, Y. Zhang. Aggregation kinetics of SDBS-dispersed carbon nanotubes in different aqueous suspensions. Colloids and Surfaces A: Physicochem. Eng. Aspects 409 (2012) 159– 166.

[105] M. D. Clark, S. Subramanian, R. Krishnamoorti. Understanding surfactant aided aqueous dispersion of multi-walled carbon nanotubes. Journal of Colloid and Interface Science 354 (2011) 144–151.

[106] B. Dong, Y. Su, Y. Liu, J. Yuan, J. Xu, L. Zheng, Dispersion of carbon nanotubes by carbazole-tailed amphiphilic imidazolium ionic liquids in aqueous solutions. Journal of Colloid and Interface Science 356 (2011) 190–195

[107] D. Douroumis, D. G. Fatouros, N. Bouropoulos, K. Papagelis, D. Tasis. Colloidal stability of carbon nanotubes in an aqueous dispersion of phospholipid. International Journal of Nanomedicine 2007:2(4) 761–766.

[108] J. Rausch, R. Zhuang, E. Mäder. Surfactant assisted dispersion of functionalized multi-walled carbon nanotubes in aqueous media. Composites: Part A 41 (2010) 1038–1046.

[109] J. Lee, M. Kim, C. K. Hong, S. E. Shim. Measurement of the dispersion stability of pristine and surface-modified multiwalled carbon nanotubes in various nonpolar and polar solvents. Meas. Sci. Technol. 18 (2007) 3707–3712.

[110] M. Loginov, N. Lebovka, E. Vorobiev. Laponite assisted dispersion of carbon nanotubes in water. Journal of Colloid and Interface Science 365 (2012) 127–136.

[111] V. Sa, K. G. Kornev. Analysis of stability of nanotube dispersions using surface tension isotherms. Langmuir 27 (2011) 13451-13460.

[112] J. Yu, N. Grossiord, C. E. Koning, J. Loos. Controlling the dispersion of multi-wall carbon nanotubes in aqueous surfactant solution. Carbon 45 (2007) 618–623.

[113] M. S. Strano, V. C. Moore, M. K. Miller, M. J. Allen, E. H. Haroz, C. Kittrell, R. H. Hauge, R. E. Smalley. The role of surfactant adsorption during ultrasonication in the dispersion of single-walled carbon nanotubes. J. Nanosci. Nanotech. 3 (2003) 81-86.

[114] A. R. Boccaccini, J. Cho, J. A. Roether, B. J. C. Thomas, E. J. Minay, M. S. P. Shaffer. Electrophoretic deposition of carbon nanotubes. Carbon 44 (2006) 3149–3160.

[115] D. Hanaor, M. Michelazzi, P. Veronesi, C. Leonelli, M. Romagnoli, C. Sorrell. Anodic Aqueous Electrophoretic Deposition of Titanium Dioxide Using Carboxylic Acids as Dispersing Agents. Journal of the European Ceramic Society 31(20116) 1041-1047.

[116] Z. Chen, Q. H. Nguyen, T. Boström. Carbon nanotube spectrally selective solar absorbers. EuroSun 2014 ISES Conference Proceedings (2014). doi:10.18086/eurosun.2014.03.05.

[117] C. Xin, C. Peng, Y. Xu, J. Wu. A novel route to prepare weather resistant, durable antireflective films for solar glass. Solar Energy 93 (2013) 121–126.

[118] R. Prodo, G. Beobide, A. Marcaide, J. Goikoetxea, A. Aranzabe. Development of multifunctional sol–gel coatings: Anti-reflection coatings with enhanced self-cleaning capacity. Solar Energy Materials & Solar Cells 94 (2010) 1081–1088.

[119] Z. Chen, A. Jain, T. Boström. Simulation of Anti-reflection coated carbonaceous spectrally selective absorbers. Energy Procedia 58 (2014) 179 – 184.

[120] T. Boström, E. Wäckelgård. Optical properties of solution-chemically derived thin film Ni–Al2O3 composites and Si, Al and Si–Ti oxides. J. Phys.: Condens. Matter 18 (2006) 7737–7750.

[121] J. Bartl, M. Baranek, Emissivity of aluminium and its importance for radiometric measurement , Meas. Sci. Rev. 4 (S3) (2004) 31-36.

[122] T. Boström, E. Wäckelgård, G. Westin. Durability tests of solution-chemically derived spectrally selective absorbers. Solar Energy Materials & Solar Cells 89 (2005) 197–207.

[123] V. Datsyuk, M. Kalyva, K. Papagelis, J. Parthenios, D. Tasis, A. Siokou, I. Kallitsis, C. Galiotis. Chemical oxidation of multiwalled carbon nanotubes. Carbon 46 (2008) 833–840.

[124] P. Karasiński, J. Jaglarz, M. Reben, E. Skoczek, J. Mazur. Porous silica xerogel films as antireflective coatings – fabrication and characterization. Optical Materials 33 (2011) 1989-1994.